Defense Nuclear Agency
Alexandria, VA 22310-3398

DNA-TR-92-140

Acoustic-Gravity Waves from Low-Altitude Localized Disturbances

Steven Bottone
Mission Research Corporation
P.O. Box 542
Newington, VA 22122-0542

May 1993

Technical Report

CONTRACT No. DNA 001-88-C-0223

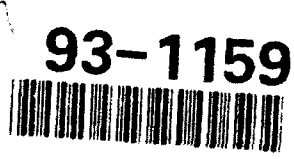

Destroy this report when it is no longer needed. Do not return to sender.

PLEASE NOTIFY THE DEFENSE NUCLEAR AGENCY, ATTN: CSTI, 6801 TELEGRAPH ROAD, ALEXANDRIA, VA 22310-3398, IF YOUR ADDRESS IS INCORRECT, IF YOU WISH IT DELETED FROM THE DISTRIBUTION LIST, OR IF THE ADDRESSEE IS NO LONGER EMPLOYED BY YOUR ORGANIZATION.

REPORT DOCUMENTATION PAGE

Form Approved OMB No. 0704-0188

1. AGENCY USE ONLY (Leave blank)	2. REPORT DATE	3. REPORT TYPE AND DATES COVERED
	930501	Technical 880923 - 921007

4. TITLE AND SUBTITLE

Acoustic-Gravity Waves from Low-Altitude Localized Disturbances

5. FUNDING NUMBERS

C - DNA 001-88-C-0223
PE - 62715H
PR - RB
TA - RB
WU - DH049280

6. AUTHOR(S)

Steven Bottone

7. PERFORMING ORGANIZATION NAME(S) AND ADDRESS(ES)

Mission Research Corporation
P.O. Box 542
Newington, VA 22122-0542

8. PERFORMING ORGANIZATION REPORT NUMBER

MRC/WDC-R-296

9. SPONSORING/MONITORING AGENCY NAME(S) AND ADDRESS(ES)

Defense Nuclear Agency
6801 Telegraph Road
Alexandria, VA 22310-3398
RAAE/Bazzoli

10. SPONSORING/MONITORING AGENCY REPORT NUMBER

DNA-TR-92-140

11. SUPPLEMENTARY NOTES

This work was sponsored by the Defense Nuclear Agency under RDT&E RMC Codes B4662D RB RB 00153 RAAE 3200A 25904D.

12a. DISTRIBUTION/AVAILABILITY STATEMENT

Approved for public release; distribution is unlimited.

12b. DISTRIBUTION CODE

13. ABSTRACT *(Maximum 200 words)*

A physics-based analytic model of the ionospheric effects of low-altitude nuclear explosions due to acoustic-gravity waves (AGW) is produced. The model contains the essence of AGW theory predictions while including basic atmospheric chemistry effects to allow descriptions of AGW induced changes for both nighttime and daytime ionospheres. The model allows multiple explosions at arbitrary times and locations although its experimental basis is, of course, from single explosion data.

14. SUBJECT TERMS

Nuclear Explosion
Ionospheric Disturbance
Acoustic-Gravity Wave
Low Altitude

15. NUMBER OF PAGES

60

16. PRICE CODE

17. SECURITY CLASSIFICATION OF REPORT	18. SECURITY CLASSIFICATION OF THIS PAGE	19. SECURITY CLASSIFICATION OF ABSTRACT	20. LIMITATION OF ABSTRACT
UNCLASSIFIED	UNCLASSIFIED	UNCLASSIFIED	SAR

CLASSIFIED BY:

N/A since Unclassified.

DECLASSIFY ON:
N/A since Unclassified.

CONVERSION TABLE

Conversion factors for U.S. Customary to metric (SI) units of measurement

MULTIPLY →	BY →	TO GET
TO GET ←	BY ←	DIVIDE

angstrom	1.000000 x E -10	meters (m)
atmosphere (normal)	1.01325 x E +2	kilo pascal (kPa)
bar	1.000000 x E +2	kilo pascal (kPa)
barn	1.000000 x E -28	meter^2 (m^2)
British thermal unit (thermochemical)	1.054350 x E +3	joule (J)
calorie (thermochemical)	4.184000	joule (J)
cal (thermochemical) / cm^2	4.184000 x E -2	mega joule/m^2 (MJ/m^2)
curie	3.700000 x E +1	*giga becquerel (GBq)
degree (angle)	1.745329 x E -2	radian (rad)
degree Farenheit	$t_K = (t_F + 459.67)/1.8$	degree kelvin (K)
electron volt	1.60219 x E -19	joule (J)
erg	1.000000 x E -7	joule (J)
erg/second	1.000000 x E -7	watt (W)
foot	3.048000 x E -1	meter (m)
foot-pound-force	1.355818	joule (J)
gallon (U.S. liquid)	3.785412 x E -3	meter^3 (m^3)
inch	2.540000 x E -2	meter (m)
jerk	1.000000 x E +9	joule (J)
joule/kilogram (J/kg) (radiation dose absorbed)	1.000000	Gray (Gy)
kilotons	4.183	terajoules
kip (1000 lbf)	4.448222 x E +3	newton (N)
kip/inch^2 (ksi)	6.894757 x E +3	kilo pascal (kPa)
ktap	1.000000 x E +2	newton-second/m^2 (N-s/m^2)
micron	1.000000 x E -6	meter (m)
mil	2.540000 x E -5	meter (m)
mile (international)	1.609344 x E +3	meter (m)
ounce	2.834952 x E -2	kilogram (kg)
pound-force (lbs avoirdupois)	4.448222	newton (N)
pound-force inch	1.129848 x E -1	newton-meter (N.m)
pound-force/inch	1.751268 x E +2	newton/meter (N/m)
pound-force/foot^2	4.788026 x E -2	kilo pascal (kPa)
pound-force/inch^2 (psi)	6.894757	kilo pascal (kPa)
pound-mass (lbm avoirdupois)	4.535924 x E -1	kilogram (kg)
pound-mass-foot^2 (moment of inertia)	4.214011 x E -2	kilogram-meter^2 (kg.m^2)
pound-mass/foot^3	1.601846 x E +1	kilogram/meter^3 (kg/m^3)
rad (radiation dose absorbed)	1.000000 x E -2	**Gray (Gy)
roentgen	2.579760 x E -4	coulomb/kilogram (C/kg)
shake	1.000000 x E -8	second (s)
slug	1.459390 x E +1	kilogram (kg)
torr (mm Hg, 0° C)	1.333220 x E -1	kilo pascal (kPa)

*The becquerel (Bq) is the SI unit of radioactivity; 1 Bq = 1 event/s.
**The Gray (Gy) is the SI unit of absorbed radiation.

TABLE OF CONTENTS

TABLE OF CONTENTS (CONTINUED)

LIST OF ILLUSTRATIONS

SECTION 1

INTRODUCTION

On 30 October 1962 the United States conducted a nuclear test of a near-surface, high-yield device, called Housatonic, which was detonated at 1600 GMT above the Pacific Ocean near Johnston Island. Observations made during this test suggested that the explosion generated a traveling ionospheric disturbance, which has been interpreted as an acoustic-gravity wave (AGW) (see reference 4). This interpretation has resulted, for the most part, from the analysis of critical frequency and virtual height measurements of vertical-incidence ionograms made at various ionosonde stations in the surrounding Pacific region. Similar observations made following the 58 MT Soviet test at Novaya Zemyla on 30 October 1961 also detected ionospheric disturbances over Europe later interpreted as produced by an acoustic-gravity wave emanating from the explosion.

Acoustic-gravity waves in the upper atmosphere can produce variations in ionospheric electron densities great enough to cause changes in the path of a high frequency (HF) signal propagating through the ionosphere. These changes, if severe enough, may disrupt HF communications in the affected regions. For the two cases mentioned above, critical frequency variations were as large as 50% and virtual height variations as large as 100 km. Such variations are not too severe in general to cause a blackout in HF communications. However, if many more similar bursts occur in a given region, and sufficiently closely spaced in time, then ionospheric electron density changes may be severe enough to cause a major disruption in HF communications. Furthermore, if enough acoustic-gravity waves produced by many low-altitude nuclear explosions interact in some region, spatial variations in ionospheric electron density with length scales on the order of 10 km may develop, which may produce enough scatter in an HF radio wave to cause an unacceptable degradation in signal strength.

This report describes a model which computes ionospheric electron density changes produced by acoustic-gravity waves generated by any number of high-yield, low-altitude nuclear explosions. The main requirement of this model is that it contain only fast-running analytic formulas possessing second order derivatives in space and time, which can also be determined and coded as analytic formulas. The implementation of this model in the RAYTRACE code, which must not be appreciably slowed-down by the AGW model, makes this requirement an absolute necessity (see the companion report, reference 6, for details on the implementation and use of the

AGW model in raytracing studies). The model is based on the linearized hydrodynamic theory of acoustic-gravity waves (see reference 2). This theory is used to justify a single burst model that fits well with the data obtained for the two events mentioned above. Section 2 provides a short description of the data, concentrating on those aspects of the data which are most important to the modeling process, while section 3 presents a thorough outline of the theory of acoustic-gravity waves. Section 4 then shows how this theory leads to predictions about hydrodynamic density changes produced in the upper atmosphere by an AGW emanating from a localized source. A comparison with the data is made at this point.

Using an entirely linear approach to compute density changes eventually leads to difficulty if either the size of an individual burst is too large or if the effects from a large number of interacting gravity waves are attempted to be computed by linear superposition of the single burst case. For a multiburst model, an approach must be taken that uses as much as possible of the single burst model but which gives reasonable results (e.g. positive densities) when the effects are combined. These issues are resolved in section 5, where a method of combining single burst effects is described.

As the number of bursts increases and ionospheric electron motions become correspondingly large, variations in electron density occur not only from volume changes produced by hydrodynamic motions, but also occur by diffusion, chemical interaction with the atmosphere, as well as solar production during daytime. Section 6 explains how these ideas are incorporated into the model. Finally, section 7 presents the final version of the model, employing the ideas described in the earlier sections. Some examples are provided to demonstrate the type of results to be expected from using the model.

SECTION 2

REVIEW OF DATA

The Housatonic device was detonated near Johnston Island at approximately 1600 GMT (4:00 a.m. local time). Variations in critical frequency of the F2 layer of the ionosphere, foF2, were observed at a number of sounding stations employing vertical-incidence ionosondes at various locations in the Pacific Ocean. Virtual height variations were also observed. These variations had the form of oscillations in the measured quantity about its ambient value, with a period of oscillation suggesting the passing of an acoustic-gravity wave. The difference in the time between the onset of these oscillations and the time of the burst, which is related to the speed at which a disturbance generated by the explosion travels to the observation point, are also consistent with a gravity wave interpretation. Details supporting these remarks are given below.

The earth's ionosphere contains free electrons with densities that vary with altitude. The ionospheric electron density generally increases with altitude until a maximum is reached in the F region, located about 300 km above the earth's surface. Vertical-incidence ionosondes can determine this maximum density, also called the peak density, by sending an electromagnetic signal, whose frequency is continuously swept from about 1 to 20 MHz (in the HF range), vertically upward into the ionosphere and measuring the time it takes the signal to return. The maximum frequency for which there is a return signal is called the critical frequency, foF2. (During daytime the F region usually has two regions with local maxima, called the F1 and F2 layers. The upper layer, which has the greatest density and remains during nighttime, is the F2 layer. The critical frequency, foF2, measures this maximum density.) The critical, or plasma, frequency of the F2 layer, foF2, is related to the peak electron density, $n_{e,\max}$, by the equation

$$\text{foF2[in MHz]} = 2.84\sqrt{n_{e,\max}[\text{in units of } 10^5 \text{ cm}^{-3}]}. \qquad (1)$$

The virtual height, h', of electrons of a given plasma frequency, is given by $h' = ct/2$, where c is the speed of light in free space and t is the time it takes the HF signal of frequency equal to the plasma frequency to reflect from those electrons and return to the ground. This is not equal to the true height of the electrons because the HF signal slows down as it travels through higher electron densities. The index of

refraction, n, of an electromagnetic wave of frequency, f, in a plasma (in the absence of collisions and magnetic field) with plasma frequency, f_p, is

$$n = \left[1 - \frac{f_p^2}{f^2}\right]^{1/2}. \tag{2}$$

It can be seen that as a wave of given frequency ($f > f_p$) encounters plasma of greater density, and hence greater plasma frequency, the index of refraction approaches zero, and the wave will reflect when $f = f_p$. The true height, h, is related to the virtual height by the integral

$$h' = \int_0^h \frac{dz}{n} = \int_0^h \frac{dz}{\sqrt{1 - n_e(z)/n_e(h)}}, \tag{3}$$

where $n_e(z)$ is the electron density as a function of altitude, z.

Figure 1 shows a plot of the critical frequency, foF2, as a function of time (GMT) above the sounding station located on the island of Tern, about 1200 km north of ground zero for Housatonic. The solid line represents the data while the dotted line shows the usual, ambient value of foF2 for those times of day. The ambient value is rising sharply at these times due to sunrise, which occurred at about 1750 GMT (5:30 a.m. local time). It is readily observed that the measured values of foF2 oscillate about the ambient value. The time of the detonation, labelled T_0, is 1600 GMT, while the first occurrence of the oscillation is about 30 minutes later. This travel time corresponds to an average speed of about .6 km/sec, which is near the average speed of sound along a line from ground zero to an observation point in the F region above Tern. Notice that the number of oscillations is about two or three before damping out and that the time elapsed between the first crest and the second crest, labelled T in the figure, is about 50 minutes. Also notice that the second oscillation appears to be broader than the first, suggesting that the period of oscillation is increasing with time.

Although not shown in the figure, the virtual height also showed some oscillation, with a decrease in virtual height corresponding to the first increase in critical frequency. As will be seen, the orientation of the earth's magnetic field lines relative to the direction of propagation of the gravity wave determines whether electrons travel up or down the field lines as the gravity wave passes. For Tern, the field lines are oriented such that electron motion down the field is expected to occur as the gravity wave first passes, as is observed (see reference 4).

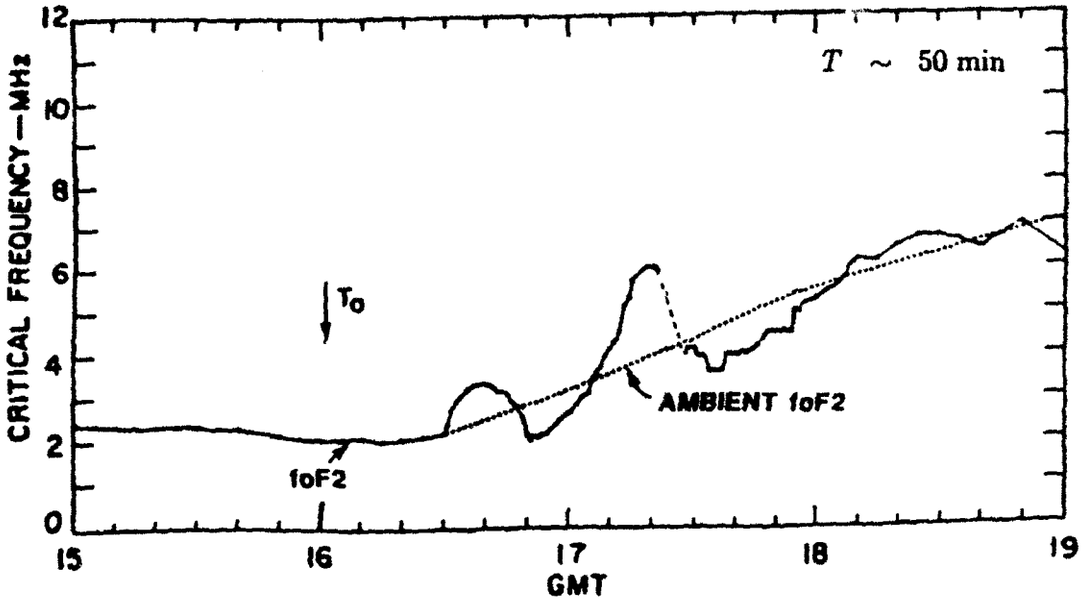

Figure 1. foF2 vs. time at Tern on 30 October 1962.

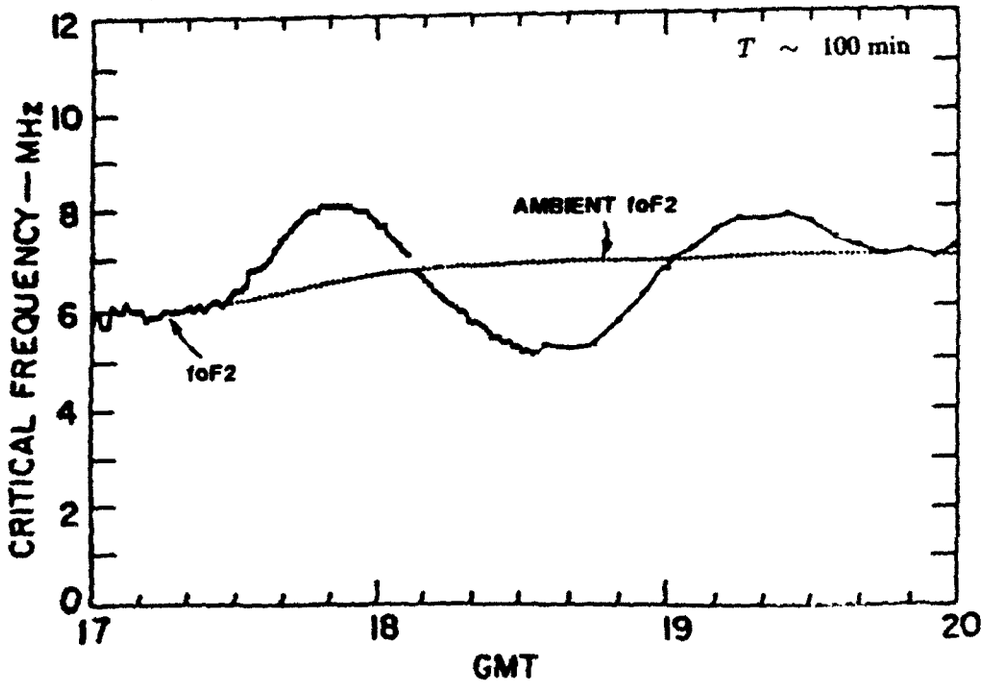

Figure 2. foF2 vs. time at Tonga on 30 October 1962.

Figure 2 shows a similar plot of the critical frequency, foF2, as a function of time (GMT) above the sounding station located on the island of Tonga, about 3900 km north of ground zero. This plot also shows an oscillation of foF2 about the ambient value. The onset time of the oscillation is about 90 minutes following the burst, which gives an average travel speed of about .7 km/sec, slightly larger than the value for Tern. The number of oscillations observed is also two or three. The time between the first crest and the second crest, labelled T, is about 100 minutes, greater than the corresponding value for Tern. As in the Tern case, the time between oscillations appears to increase with time. Finally, the relative change in foF2 with respect to ambient, as measured by the amplitude of the first oscillation, is smaller for the Tonga data than for the Tern data. As for Tern, the virtual height decreases initially, as is expected from the orientation of the earth's magnetic field above Tonga. Although these two sites provided the cleanest data, similar variations in foF2 were observed at other locations, the details of which can be obtained in reference 4.

Figure 3 shows plots of the critical frequency, foF2, as a function of time (MET) above various European sounding stations, following the 58 MT Soviet test at Novaya Zemyla on 30 October 1961. The stations shown in the figure are located at increasing distance from ground zero going up in the figure, from about 1400 km for Kiruna to about 4300 km for Athens. Although the data used to make the figure were not very good, some general observations can be made. The most obvious characteristic is that the period of oscillation increases with increasing distance from ground zero. It is also seen that the number of oscillations at most locations is about four or five. A careful examination also shows that there was an initial decrease in foF2, with a corresponding increase in virtual height (not shown in the figure), which is expected from the magnetic field orientation at those sites. It is not clear from the figure whether or not there is much decrease in the amplitude of the oscillations with increasing distance from ground zero.

The data shows a number of features which will be important in constructing an acoustic-gravity wave model. The most important general feature is that the F region of the ionosphere oscillates at quite distant points following a large, near-surface explosion. The period of oscillation increases with increasing distance from the source, approximately linearly with distance. The period of oscillation at any given point also increases slightly with time. The number of oscillations is approximately constant for a given burst, independent of location. The amplitude of the oscillation decreases with distance, although the data are insufficient to determine what the scaling law with distance is. The direction of ionospheric electron motion depends on the orientation of the earth's magnetic field lines with respect to the direction of propagation of the gravity wave. In section 4 it will be shown how the general theory

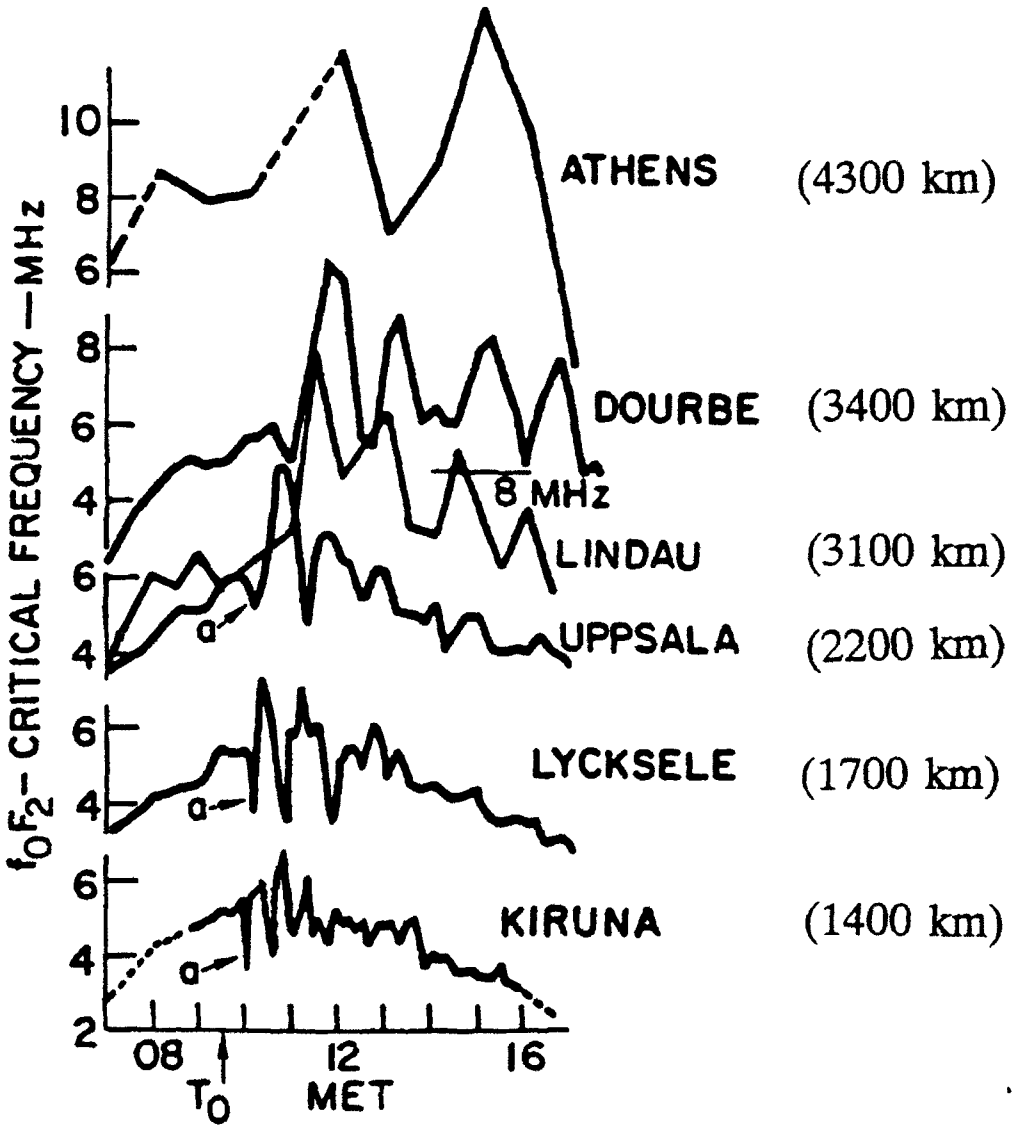

Figure 3. foF2 vs. time at various European stations on 30 October 1961.

of acoustic-gravity waves can be used to derive these properties, which will be the basis for constructing the AGW model. Before presenting these derivations, a review of the general theory of acoustic-gravity waves will be presented in section 3.

SECTION 3

THEORY OF ACOUSTIC-GRAVITY WAVES

Most properties of acoustic-gravity waves, in particular those discussed in the previous chapter, can be derived by assuming that the earth's atmosphere can be described as a stationary, stratified fluid, with constant temperature in a uniform gravitational field. Acoustic-gravity waves come about as small (first order) perturbations about isothermal equilibrium of the equations of hydrodynamics. The fluid is described by the pressure, p, density ρ, and velocity $\mathbf{v}$, given as functions of position and time. The equations of motion are the equation of continuity, balance of linear momentum, and adiabatic equation, given, respectively, by

$$\frac{D\rho}{Dt} + \rho\nabla \cdot \mathbf{v} = 0, \tag{4}$$

$$\rho\frac{D\mathbf{v}}{Dt} + \nabla p = \rho\mathbf{g}, \tag{5}$$

$$\frac{Dp}{Dt} + \gamma p\nabla \cdot \mathbf{v} = 0, \tag{6}$$

where the convective derivative is given by $D/Dt \equiv \partial/\partial t + \mathbf{v} \cdot \nabla$, γ is the adiabatic constant, and gravity is assumed to be constant in the negative z direction, $\mathbf{g} = -g\hat{\mathbf{e}}_z$. Equation (6) is derived by assuming the specific entropy of a material particle, s, is constant,

$$\frac{Ds}{Dt} = 0, \tag{7}$$

and that the fluid is ideal (or perfect),

$$s = c_v \ln\frac{p}{\rho^\gamma}, \tag{8}$$

and using the continuity equation (4).

The density of a fluid in static, motionless ($\mathbf{v} = 0$), isothermal equilibrium is distributed exponentially as a function of height,

$$\rho^{(0)} = \rho_0 e^{-z/H}, \tag{9}$$

where ρ_0 is the density at $z = 0$. The corresponding pressure is

$$p^{(0)} = p_0 e^{-z/H}. \tag{10}$$

According to equation (5) the constants ρ_0 and p_0 must be related to the scale height, H, by

$$p_0 = \rho_0 g H. \tag{11}$$

The speed of sound, c, is given by

$$c^2 = \gamma \frac{p}{\rho} = \gamma \frac{p_0}{\rho_0} = \gamma g H. \tag{12}$$

To derive the linearized equations of motion from equations (4)–(6), which describe small perturbations about the solutions given by equations (11) and (12) (with $\mathbf{v}^{(0)} = 0$), we will use perturbation theory in a systematic way so the interested reader may use this approach as a starting point for higher order corrections, which will not be pursued here. It is easiest to work in cartesian coordinates and suppress the y component of the velocity, which can be included at any point in what follows by making the obvious changes. Therefore, let the velocity, $\mathbf{v}$, be written

$$\mathbf{v}(x, z, t) = u(x, z, t)\hat{\mathbf{e}}_x + w(x, z, t)\hat{\mathbf{e}}_z. \tag{13}$$

The equations of motion in component form are

$$\frac{\partial \rho}{\partial t} + u\frac{\partial \rho}{\partial x} + w\frac{\partial \rho}{\partial z} + \rho\frac{\partial u}{\partial x} + \rho\frac{\partial w}{\partial z} = 0, \tag{14}$$

$$\frac{\partial u}{\partial t} + u\frac{\partial u}{\partial x} + w\frac{\partial u}{\partial z} + \frac{1}{\rho}\frac{\partial p}{\partial x} = 0, \tag{15}$$

$$\frac{\partial w}{\partial t} + u\frac{\partial w}{\partial x} + w\frac{\partial w}{\partial z} + \frac{1}{\rho}\frac{\partial p}{\partial z} = -g, \tag{16}$$

$$\frac{\partial p}{\partial t} + u\frac{\partial p}{\partial x} + w\frac{\partial p}{\partial z} + \gamma p\frac{\partial u}{\partial x} + \gamma p\frac{\partial w}{\partial z} = 0. \tag{17}$$

A solution to these equations is assumed in the form of an expansion in powers of the perturbation parameter, ϵ,

$$u(x,z,t) = \epsilon u^{(1)}(x,z,t) + \epsilon^2 u^{(2)}(x,z,t) + \cdots, \tag{18}$$

$$w(x,z,t) = \epsilon w^{(1)}(x,z,t) + \epsilon^2 w^{(2)}(x,z,t) + \cdots, \tag{19}$$

$$\rho(x,z,t) = \rho^{(0)} + \epsilon\rho^{(1)}(x,z,t) + \epsilon^2\rho^{(2)}(x,z,t) + \cdots, \tag{20}$$

$$p(x,z,t) = p^{(0)} + \epsilon p^{(1)}(x,z,t) + \epsilon^2 p^{(2)}(x,z,t) + \cdots, \tag{21}$$

where $\rho^{(0)}$ and $p^{(0)}$ are given in equations (9) and (10). Also needed is the expansion for the function ρ^{-1},

$$\rho^{-1} = \frac{1}{\rho^{(0)}}\left(1 - \epsilon\frac{\rho^{(1)}}{\rho^{(0)}} - \epsilon^2\frac{\rho^{(2)}}{\rho^{(0)}} + \epsilon^2\left(\frac{\rho^{(1)}}{\rho^{(0)}}\right)^2 + \cdots\right). \tag{22}$$

Substitution of equations (18) to (22) into equation (14) and using the condensed notation, $u_x \equiv \partial u/\partial x$, gives

$$\begin{aligned}
&\epsilon\rho_t^{(1)} + \epsilon^2\rho_t^{(2)} + \cdots + \left(\epsilon u^{(1)} + \cdots\right)\left(\epsilon\rho_x^{(1)} + \cdots\right) + \\
&\left(\epsilon w^{(1)} + \epsilon^2 w^{(2)} + \cdots\right)\left(\rho_z^{(0)} + \epsilon\rho_z^{(1)} + \cdots\right) + \\
&\left(\rho^{(0)} + \epsilon\rho^{(1)} + \cdots\right)\left(\epsilon u_x^{(1)} + \epsilon w_z^{(1)} + \epsilon^2 u_x^{(2)} + \epsilon^2 w_z^{(2)} + \cdots\right) = 0.
\end{aligned} \tag{23}$$

Collecting terms in like powers of ϵ gives

$$\varepsilon\left(\rho_t^{(1)} + w^{(1)}\rho_z^{(0)} + \rho^{(0)}u_x^{(1)} + \rho^{(0)}w_z^{(1)}\right) +$$
$$\varepsilon^2\left(\rho_t^{(2)} + u^{(1)}\rho_x^{(1)}w^{(2)}\rho_z^{(0)} + w^{(1)}\rho_z^{(1)} + \rho^{(0)}u_x^{(2)} + \rho^{(0)}w_z^{(2)} + \rho^{(1)}u_x^{(1)} + \rho^{(1)}w_z^{(1)}\right)$$
$$+ \cdots = 0. \tag{24}$$

Substitution of equations (18) to (22) into equations (15)–(17) produces three more equations similar to equation (24). Setting the coefficient of each power of ε equal to zero and assembling the sets of equations that result order by order yields through second order,

Zeroth order:

$$p_z^{(0)} = -\rho^{(0)}g, \tag{25}$$

from which it can be concluded that $p_0 = \rho_0 gH$ as in equation (11).

First order:

$$\rho_t^{(1)} + w^{(1)}\rho_z^{(0)} + \rho^{(0)}u_x^{(1)} + \rho^{(0)}w_z^{(1)} = 0, \tag{26}$$

$$u_t^{(1)} + \frac{1}{\rho^{(0)}}p_x^{(1)} = 0, \tag{27}$$

$$w_t^{(1)} + \frac{1}{\rho^{(0)}}p_z^{(1)} - \frac{1}{\rho^{(0)}}\frac{\rho^{(1)}}{\rho^{(0)}}p_z^{(0)} = 0, \tag{28}$$

$$p_t^{(1)} + w^{(1)}p_z^{(0)} + \gamma p^{(0)}u_x^{(1)} + \gamma p^{(0)}w_z^{(1)} = 0, \tag{29}$$

which are the usual linear AGW equations.

Second order:

$$\rho_t^{(2)} + w^{(2)}\rho_z^{(0)} + \rho^{(0)}u_x^{(2)} + \rho^{(0)}w_z^{(2)} = -u^{(1)}\rho_x^{(1)} - w^{(1)}\rho_z^{(1)} - \rho^{(1)}u_x^{(1)} + \rho^{(1)}w_z^{(1)}, \tag{30}$$

$$u_t^{(2)} + \frac{1}{\rho^{(0)}} p_x^{(2)} = -u^{(1)} u_x^{(1)} - w^{(1)} u_z^{(1)} + \frac{1}{\rho^{(0)}} \frac{\rho^{(1)}}{\rho^{(0)}} p_x^{(1)}, \tag{31}$$

$$w_t^{(2)} + \frac{1}{\rho^{(0)}} p_z^{(2)} - \frac{1}{\rho^{(0)}} \frac{\rho^{(2)}}{\rho^{(0)}} p_z^{(0)} = -u^{(1)} w_x^{(1)} - w^{(1)} w_z^{(1)} + \frac{1}{\rho^{(0)}} \frac{\rho^{(1)}}{\rho^{(0)}} p_z^{(1)} - \frac{1}{\rho^{(0)}} \left(\frac{\rho^{(1)}}{\rho^{(0)}} \right)^2 p_z^{(0)}, \tag{32}$$

$$p_t^{(2)} + w^{(2)} p_z^{(0)} + \gamma p^{(0)} u_x^{(2)} + \gamma p^{(0)} w_z^{(2)} = -u^{(1)} p_x^{(1)} - w^{(1)} p_z^{(1)} - \gamma p^{(1)} u_x^{(1)} + \gamma p^{(1)} w_z^{(1)}, \tag{33}$$

which are also linear equations in the second order quantities appearing on the left hand sides. The functions on the right hand sides are of no greater than first order and are to be considered given solutions of the first order equations. The second order equations are given here for reference, they will not be needed in what follows. As a check on the expansions, it will be seen that the sum of the superscripts of each term is equal to the order of the expansion.

We will now focus our attention on the linear AGW equations (26)–(29). Solutions of these equations, subject to appropriate initial and boundary conditions, describe the motion of small disturbances from the equilibrium configuration given by equations (9) and (10). If the disturbance is too large, then these equations do not provide an adequate description and higher order corrections or an entirely different approach are needed. It has been found that the linear AGW equations usually provide an adequate description of traveling ionosphere disturbances at points distant from the source of the wave. In our case, we wish to describe ionospheric motion at points far from and at greater altitudes of a point which is the source of a large localized atmospheric disturbance. The linear equations will not yield solutions at points near the source. Eventually, however, the disturbance will have spread out enough that an initial configuration can be defined which is close to the linear regime. The difficultly, of course, is that this initial configuration is unknown. It will be seen, however, that much information is revealed by making quite general assumptions about this initial configuration and employing general plane wave solutions of the linear equations, which will now be described.

It can be shown that plane solutions to equations (26)–(29) exist if an exponential factor with scale height $2H$ is added to the velocity functions and exponential factors with scale height $-2H$ are added to the density and pressure changes (see, for example, reference 8). That is, there exist solutions of the form

$$u_{\mathbf{k}}^{(1)}(\mathbf{r},t) = u_1(\mathbf{k})\, e^{z/2H}\, e^{i(\mathbf{k}\cdot\mathbf{r} - \omega(\mathbf{k})t)}, \tag{34}$$

$$w_{\mathbf{k}}^{(1)}(\mathbf{r},t) = w_1(\mathbf{k})\, e^{z/2H}\, e^{i(\mathbf{k}\cdot\mathbf{r} - \omega(\mathbf{k})t)}, \tag{35}$$

$$\rho_{\mathbf{k}}^{(1)}(\mathbf{r},t) = \rho_1(\mathbf{k})\, e^{-z/2H}\, e^{i(\mathbf{k}\cdot\mathbf{r} - \omega(\mathbf{k})t)}, \tag{36}$$

$$p_{\mathbf{k}}^{(1)}(\mathbf{r},t) = p_1(\mathbf{k})\, e^{-z/2H}\, e^{i(\mathbf{k}\cdot\mathbf{r} - \omega(\mathbf{k})t)}. \tag{37}$$

Here, the complex constants, u_1, w_1, ρ_1, and p_1, depend only on the wave number $\mathbf{k}$ and provide the relative amplitude and phase of the first order perturbations. Their precise form can be determined in a straightforward manner, but will not be needed here (see reference 8 for details). The angular frequency, $\omega(\mathbf{k})$, is determined by the dispersion relation

$$k_z^2 = k_h^2\left(\frac{\omega_b^2}{\omega^2} - 1\right) + \frac{1}{c^2}\left(\omega^2 - \omega_a^2\right) \tag{38}$$

where k_h stands for the horizontal wave number which is k_x for the planar case where there is no y dependence or $k_h^2 = k_x^2 + k_y^2$ for the general or radially symmetric case, which will be the case in the subsequent presentation. The acoustic cutoff frequency, ω_a, and the Brunt-Väisälä frequency, ω_b, are given by

$$\omega_a^2 = \left(\frac{\gamma g}{2c}\right)^2, \qquad \omega_b^2 = (\gamma - 1)\,\frac{g^2}{c^2}. \tag{39}$$

The dispersion relation (38) can also be written

$$\omega^2 = \frac{1}{2}\left(c^2k^2 + \omega_a^2\right) \pm \frac{1}{2}\sqrt{\left(c^2k^2 + \omega_a^2\right)^2 - 4c^2k_h^2\omega_b^2}. \tag{40}$$

It is easy to show from this equation that waves can propagate ($\omega^2 > 0$) only if $\omega > \omega_a$, which is called the acoustic branch, or $\omega < \omega_b$, which is called the gravity wave branch. In the subsequent analysis, most of our concern will be with waves that are composed

of solutions whose frequencies are in the gravity wave branch and we will use the term gravity wave to describe such solutions.

A general solution to equations (26)–(29) can be obtained as a superposition of the plane wave solutions (34)–(37). For example, the horizontal velocity $u(\mathbf{r},t)$ can be written

$$\begin{aligned} u(\mathbf{r},t) &= \frac{1}{(2\pi)^{3/2}} \int \tilde{f}(\mathbf{k}) u_{\mathbf{k}}^{(1)}(\mathbf{r},t)\, d\mathbf{k} \\ &= \frac{e^{z/2H}}{(2\pi)^{3/2}} \int \tilde{f}(\mathbf{k}) u_1(\mathbf{k}) e^{i\mathbf{k}\cdot\mathbf{r}} e^{-i\omega(\mathbf{k})t}\, d\mathbf{k}. \end{aligned} \tag{41}$$

If the initial condition for u is (the initial condition for the function u is the horizontal velocity as a function of position following the onset of the localized disturbance at some later time, which will be taken as $t = 0$, such that the disturbance is small enough so that the linear approximation is valid)

$$u(\mathbf{r},0) = f(\mathbf{r}), \tag{42}$$

then a straightforward application of the Fourier theorem shows that

$$\tilde{f}(\mathbf{k}) = \frac{1}{(2\pi)^{3/2}} \frac{1}{u_1(\mathbf{k})} \int f(\mathbf{r}) e^{-z/2H} e^{-i\mathbf{k}\cdot\mathbf{r}}\, d\mathbf{r}. \tag{43}$$

The initial conditions can be used to determine the parameter ϵ, usually taken to be one.

With a few simple assumptions regarding the nature of the function $\tilde{f}(\mathbf{k})$, a great deal can be learned by studying equation (41) and using the dispersion relation (38), which is the subject of the next section.

SECTION 4

ASYMPTOTIC ANALYSIS OF GRAVITY WAVES

By applying standard asymptotic analysis to integral solutions of the AGW equations such as that appearing in equation (41), a great deal can be learned about the nature of the solutions at positions far from a localized initial disturbance for late times. It will be seen that much of the information can be obtained from the dispersion relation independent of the precise details of the initial conditions. In particular, the method of stationary phase will be used, which can be stated as follows: let

$$I(\lambda) = \int f(\mathbf{x}) \exp[i\lambda\phi(\mathbf{x})]\, d\mathbf{x}, \qquad \mathbf{x} = (x_1, \ldots, x_n). \tag{44}$$

Under suitable conditions, which can be found in reference 1, this integral can be expanded in an asymptotic expansion for $\lambda \to \infty$, the first term of which is

$$I(\lambda) \sim \left(\frac{2\pi}{\lambda}\right)^{n/2} \sum \frac{f(\mathbf{x}_0) \exp\left[i\lambda\phi(\mathbf{x}_0) + i\frac{\pi}{4}\mathrm{sgn}\det\left(\phi_{x_i x_j}(\mathbf{x}_0)\right)\right]}{\left|\det\left(\phi_{x_i x_j}(\mathbf{x}_0)\right)\right|^{1/2}}, \tag{45}$$

where the sum is over all those points, $\mathbf{x}_0$, such that $\nabla\phi(\mathbf{x}_0) = 0$. Higher order terms contain larger negative powers of λ, which approach zero faster than the term above as $\lambda \to \infty$.

Applying this well-known result to equation (41) provides an asymptotic approximation for the horizontal velocity, and similarly for the other hydrodynamic field variables, as $t \to \infty$,

$$u(\mathbf{r},t) \sim e^{z/2H} \frac{\tilde{f}(\mathbf{k}_0) u_1(\mathbf{k}_0) \exp\left[i\left(\mathbf{k}_0 \cdot \mathbf{r} - \omega(\mathbf{k}_0)t\right) + i\frac{\pi}{4}\mathrm{sgn}\det\left(\frac{\partial^2\omega(\mathbf{k}_0)}{\partial k_i \partial k_j}\right)\right]}{t^{3/2}\left|\det\left(\frac{\partial^2\omega(\mathbf{k}_0)}{\partial k_i \partial k_j}\right)\right|^{1/2}}, \tag{46}$$

where $\mathbf{k}_0$ is a solution of

$$\frac{\partial \omega}{\partial k_h} = \frac{r_h}{t}, \qquad \frac{\partial \omega}{\partial k_z} = \frac{z}{t}, \tag{47}$$

with $r_h^2 = x^2 + y^2$ and $k_h^2 = k_x^2 + k_y^2$.

4.1 FREQUENCY OF OSCILLATION.

To solve equations (47) to determine $\omega_0 = \omega(\mathbf{k}_0)$ we use the dispersion relation (38) to obtain

$$\frac{\partial \omega}{\partial k_h} = -\frac{k_h\left(\frac{\omega_b^2}{\omega^2} - 1\right)}{-\frac{k_h^2\omega_b^2}{\omega^3} + \frac{\omega}{c^2}}, \qquad \frac{\partial \omega}{\partial k_z} = \frac{k_z}{-\frac{k_h^2\omega_b^2}{\omega^3} + \frac{\omega}{c^2}}. \tag{48}$$

Using these relations in equation (47) and taking the ratio of the second to the first equation gives

$$-\frac{k_z}{k_h\left(\frac{\omega_b^2}{\omega^2} - 1\right)} = \frac{1}{\tan\theta}, \tag{49}$$

where $\cos\theta = z/r$, $r^2 = r_h^2 + z^2$. From this and the dispersion relation it follows that

$$k_h^2 = \frac{\omega^2 - \omega_a^2}{c^2}\,\frac{\omega^4 \sin^2\theta}{\left(\omega^2 - \omega_b^2\right)\left(\omega^2 - \omega_b^2\cos^2\theta\right)}, \tag{50}$$

$$k_z^2 = \frac{\omega^2 - \omega_a^2}{c^2}\,\frac{\left(\omega^2 - \omega_b^2\right)\cos^2\theta}{\left(\omega^2 - \omega_b^2\cos^2\theta\right)}. \tag{51}$$

Taking the sum of the squares of equations (47) gives

$$\frac{k_h^2 \frac{1}{\omega^4}\left(\omega^2-\omega_b^2\right)^2 + k_z^2}{\frac{1}{\omega^2}\left(\frac{\omega^2}{c^2} - k_h^2\frac{\omega_b^2}{\omega^2}\right)} = \frac{r^2}{t^2}. \tag{52}$$

Using equations (50) and (51) in this equation finally yields

$$\frac{\left(\omega^2-\omega_a^2\right)\left(\omega^2-\omega_b^2\right)^3\left(\omega^2-\omega_b^2\cos^2\theta\right)}{\omega^2\left[\left(\omega^2-\omega_b^2\right)\left(\omega^2-\omega_b^2\cos^2\theta\right)-\left(\omega^2-\omega_a^2\right)\left(\omega_b^2\sin^2\theta\right)\right]^2} = \frac{r^2}{c^2t^2}. \tag{53}$$

The solution(s) of this equation give(s) those frequencies, ω_0, to be used in the asymptotic solution (46), which we will now analyze.

Let the square root of the left hand side of the above equation be designated $f(\omega)$ so the equation is written

$$f(\omega) = \frac{r}{ct}. \tag{54}$$

Solution of this equation can be obtained in a graphical manner as shown in figure 4. The solid curve in the figure is a plot of $1/f(\omega)$ as a function of ω/ω_b. The horizontal dashed line has an ordinate equal to $\tau = ct/r$. Solutions of equation (53) are at those points where the two curves intersect. It can be readily seen that for t large enough there are three solutions, which will be called $\omega_{0,1}$, $\omega_{0,2}$, and $\omega_{0,3}$. It is obvious from equation (53), that as $t \to \infty$,

$$\omega_{0,1} \to \omega_c, \qquad \omega_{0,2} \to \omega_b, \qquad \omega_{0,3} \to \omega_a, \tag{55}$$

where $\omega_c \equiv \omega_b \cos\theta$.

Low frequency gravity wave oscillations whose frequency approaches ω_c are consistent with observations. For observation locations at equal altitudes, the frequency, ω_c, decreases with distance from the localized source as $1/r$, as is observed. It also is clear from figure 4 that as $t \to \infty$, $\omega_0 \to \omega_c$ (from this point we will be concerned only with $\omega_{0,1}$ which will be called ω_0) from above, that is, the oscillation frequency decreases with time (the period increases) as is also observed. To the next order in t it can be shown that

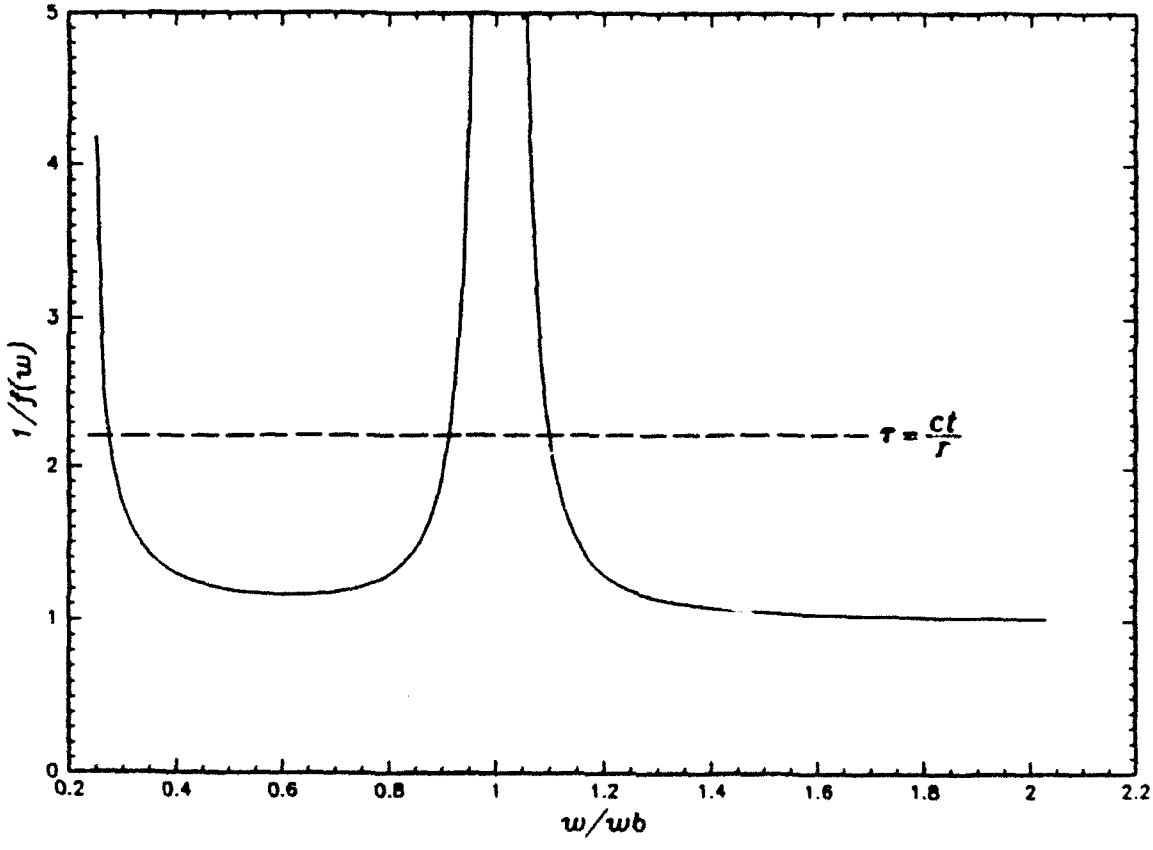

Figure 4. Graphical solution for asymptotic frequency.

$$\omega_0 \sim \omega_c \left(1 + \frac{1}{2}\frac{r^2}{\tilde{c}^2 t^2}\right), \tag{56}$$

where $\tilde{c} = (\omega_b/\omega_a)c$, which for a typical atmosphere, is a speed just slightly less than c.

4.2 SCALING WITH DISTANCE.

The asymptotic solution for the horizontal velocity given be equation (46) is an oscillatory function of time whose frequency approaches ω_c as $t \to \infty$. Using equations (50) and (51) it follows that

$$\mathbf{k}\cdot\mathbf{r} = \frac{r}{c}\sqrt{\frac{\left(\omega^2 - \omega_a^2\right)\left(\omega^2 - \omega_c^2\right)}{\left(\omega^2 - \omega_b^2\right)}}, \tag{57}$$

which approaches zero as $t \to \infty$, showing there is no spatial oscillation at late times.

The amplitude of the oscillation (suppressing the $\exp(z/2H)$ factor), which will be called u_0, is then

$$u_0(\mathbf{r},t) \sim \frac{\tilde{f}(k_0)u_1(\mathbf{k}_0)}{t^{3/2}\left|\det\left(\dfrac{\partial^2\omega(\mathbf{k}_0)}{\partial k_i \partial k_j}\right)\right|^{1/2}}, \tag{58}$$

where we have assumed $\tilde{f}$ is spherically symmetric and written its argument as k_0. A bit of arithmetic shows that asymptotically as $t \to \infty$

$$k_{z,0} \sim \frac{\omega_b t}{r}, \qquad k_{h,0} \sim -\omega_b t\frac{z}{r^2}, \tag{59}$$

which gives

$$k_0 \sim \frac{\omega_b t}{r}, \qquad \omega_0 \sim \frac{z}{r}\omega_b. \tag{60}$$

It can also be shown that

$$\det\left(\frac{\partial^2\omega}{\partial k_i \partial k_j}\right) \sim \frac{\omega_b^3}{k_{h,0} k_{z,0}^5}, \tag{61}$$

from which it follows that

$$\left|\det\left(\frac{\partial^2\omega}{\partial k_i \partial k_j}\right)\right|^{-1/2} \sim \omega_b^{3/2} \left(\frac{t}{r}\right)^3 \left(\frac{z}{r}\right)^{1/2}. \tag{62}$$

Finally, $u_1 \sim 1$ and, therefore, the scaling relation for u_0 is,

$$u_0(\mathbf{r}, t) \sim \frac{1}{t^{3/2}} \left(\frac{t}{r}\right)^3 \left(\frac{z}{r}\right)^{1/2} \tilde{f}\left(\frac{w_b t}{r}\right), \tag{63}$$

Consider now some point, call it t_0, in the oscillation where m cycles have occurred (m may be a fraction), then

$$\omega_0 t_0 = 2\pi m \qquad \text{or} \qquad t_0 = \frac{2\pi m}{\omega_b} \frac{r}{z}, \tag{64}$$

from which it follows that

$$u_0(\mathbf{r}, t_0) \sim \frac{1}{r^2} \tilde{f}\left(\frac{2\pi m}{z}\right). \tag{65}$$

This equation shows that for points at altitude, z, the number of oscillations, m, which occur is the same independent of the distance from the localized source, r, if $\tilde{f}$ is a function of finite width, which is the case for a finite sized initial disturbance. This equation also shows that the amplitude of the oscillations, for a given number of oscillations, scales with distance as $1/r^2$.

4.3 TIME OF ONSET.

It is well known that wave energy travels at the group velocity,

$$\mathbf{v}_g = \frac{\partial \omega}{\partial \mathbf{k}}. \tag{66}$$

For acoustic-gravity waves this value is bounded by the speed of sound, c. This means that if a disturbance is localized, then an undisturbed point will remain so until a time equal to r/c has elapsed, where r is the distance between the undisturbed point and the closest point of the disturbance. If disturbances are confined to the gravity wave branch ($\omega < \omega_b$), then the travel is speed is actually bounded by $\tilde{c} = (\omega_b/\omega_a)c$. To see this, note that for horizontal propagation, which is the fastest way to cover a distance R, the dispersion relation shows the horizontal component of the group velocity, u_g, can be written

$$u_g = \left[\frac{\omega^2 - \omega_a^2}{\omega^2 - \omega_b^2}\right]^{1/2} \frac{\left(\omega^2 - \omega_b^2\right)^2}{\left(\omega^2 - \omega_b^2\right)^2 + \omega_b^2\left(\omega_a^2 - \omega_b^2\right)} c. \tag{67}$$

For $\omega < \omega_b$ this equation shows that u_g has a maximum equal to $\tilde{c}$ for $\omega = 0$. Therefore, for an initial disturbance that is localized at the origin at $t = 0$, the soonest a gravity wave disturbance can reach a point located at a distant r, assumed to be large compared to the extent initial disturbance, is about $t = r/\tilde{c}$.

4.4 ELECTRON DENSITY CHANGES.

Up to this point we have concentrated our attention on the horizontal component of the neutral velocity of the atmosphere during the passage of an acoustic-gravity wave (it can be shown that the vertical velocity component is smaller by a factor of $1/r$ asymptotically). Measurable changes in the ionosphere are produced by indirect coupling of the ionospheric electrons to the neutral motion of the atmosphere. It can be demonstrated that at F-region altitudes the coupling is such that the electron velocity is equal to the ionic velocity, $\mathbf{v}_i$, which is equal to the component of the neutral velocity along the earth's magnetic field, i.e.

$$\mathbf{v}_i = (\mathbf{v} \cdot \hat{\mathbf{B}})\,\hat{\mathbf{B}}, \tag{68}$$

where $\hat{\mathbf{B}}$ is a unit vector in the direction of the earth's magnetic field. (Full justification of this relation can be found in reference 3.) Let the electron density change, to first order, be denoted n' so that the electron density is given by

$$n_e(\mathbf{r},t) = n_0(z) + n'(\mathbf{r},t), \tag{69}$$

where n_0 is the ambient electron density, assumed to be stratified. The first order continuity equation for electrons is then

$$\frac{\partial n'}{\partial t} + \nabla \cdot (n_0 \mathbf{v}_i) = 0. \tag{70}$$

For a realistic atmosphere, dissipation of gravity waves occur as it propagates vertically upwards, due to ion drag, viscosity, and heat conduction. Attenuation of the wave begins to occur at approximately F-region heights in such a way that the $\exp(z/2H)$ increase in the neutral velocity is almost exactly cancelled at greater heights (see references 5 and 9). Therefore, let the form of the neutral velocity at F-region heights be

$$\mathbf{v} = \mathbf{v}_0 e^{i(\mathbf{k}\cdot\mathbf{r} - \omega t)}. \tag{71}$$

Assuming the same time dependence for n', equation (70) gives

$$n' = -\frac{1}{\omega}(\mathbf{v}\cdot\hat{\mathbf{B}})\left[(\mathbf{k}\cdot\hat{\mathbf{B}})n_0 + i(\hat{\mathbf{e}}_z\cdot\hat{\mathbf{B}})\frac{\partial n_0}{\partial z}\right]. \tag{72}$$

At the electron density peak, where $\partial n_0/\partial z = 0$, it can be seen that the electron density change is in phase with the neutral velocity, the density increasing for electrons moving downward and decreasing for electrons moving upward. Applying the asymptotic scaling relations, equations (58)–(65), we have for the scaling relation with distance for the amplitude of n' at the peak

$$n'(\mathbf{r},t_0) \sim K\frac{1}{r}\tilde{f}\left(\frac{2\pi m}{z}\right), \tag{73}$$

where K is a constant that depends on the magnetic field orientation, ω_b, and the point in the oscillation of concern (usually the peak). Notice that the amplitude of the oscillations, for a fixed peak altitude, falls off as $1/r$, which is consistent with the data for ranges that are not too long.

4.5 COMPARISON WITH DATA.

At this point we have derived enough characteristics of gravity waves emanating from a localized source to construct a simple model that agrees well with the data presented in section 2. To do this we must choose a form for the unknown function, $\tilde{f}$, which is related to the initial distribution of the hydrodynamic horizontal velocity. As explained above, the form of the function determines the number of oscillations as well as the magnitude of the amplitude, expected to be different for each initial disturbance. The frequency of oscillation, onset time, and scaling do not. We will try a simple function of finite width, a guassian of the form

$$\tilde{f}(k) = U \exp\left(-\frac{k^2}{a^2}\right), \tag{74}$$

with

$$a = \frac{2\pi m}{z}, \tag{75}$$

where the constants U and m are expected to depend on the total energy of the initial configuration. We will make a fit to the data to determine these constants.

In order to account for free electrons created by solar radiation, as seen in the data in figures 1 and 2, we simply add a constant source term for electrons, $Q(t)$ to the right hand side of equation (72) which agrees with the ambient data when no gravity waves are present. With this in mind, a simple numerical solution of equation (72) the horizontal neutral velocity of section 4.1, the onset time determined in section 4.3, and the function $\tilde{f}$ given by equation (74) with the constants suitably adjusted, produces the critical frequency changes plotted in figures 5 and 6. The dashed lines correspond to data plotted in figure 1 and 2, while the solid lines are the results of the model. As can be seen by in the figures, the model reproduces the essential features of the data.

Comparison with the Soviet test data allows a scaling relation with yield for the amplitude U and the parameter m which gives the number of oscillations to be determined. It is found that reasonable fits result from

$$U = U_0 Y, \qquad m = m_0 \sqrt{Y} \tag{76}$$

where the values of the constants are determined by a best fit to the data.

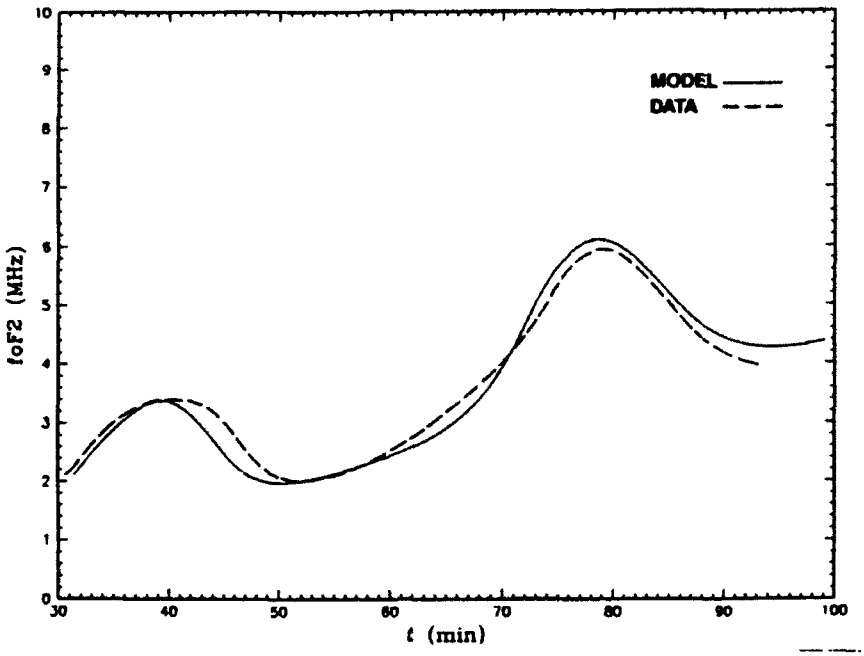

Figure 5. Comparison of model with data for foF2 vs. time at Tern on 30 October 1962.

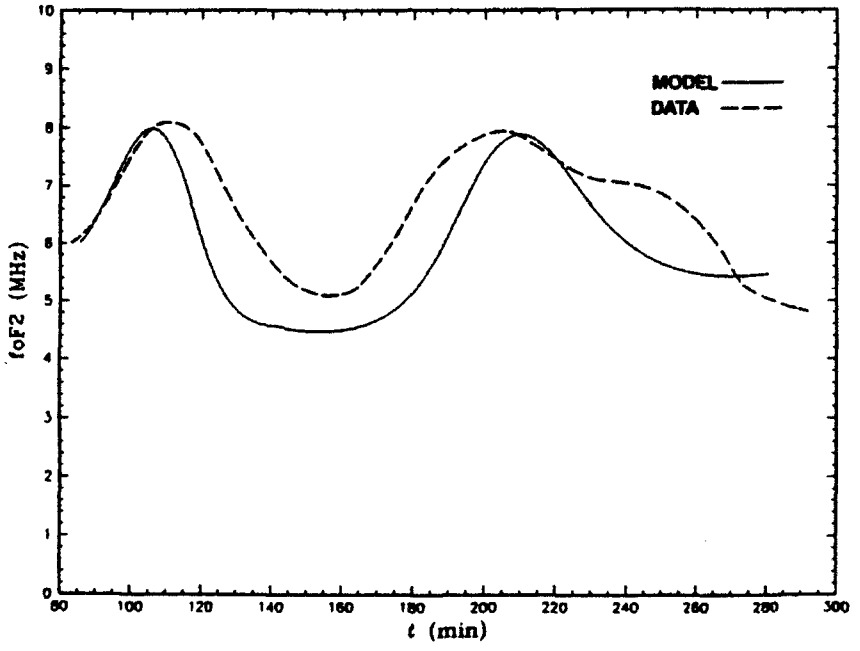

Figure 6. Comparison of model with data for foF2 vs. time at Tonga on 30 October 1962.

SECTION 5

NONLINEAR ISSUES

Electron density changes as computed by equations (70) or (72) are valid only under the approximation that the change n' is small compared to the ambient electron density n_e. The electron density changes depend on the horizontal neutral velocity, given asymptotically in equation (46). The magnitude of this velocity is determined implicitly by the function $\tilde{f}$ which, in turn, depends on the magnitude of the initial condition, as given in equation (42). If this velocity is large compared with the speed of sound, then the approximation which shows that the solution of the linear first order equations (26)–(29) are close to the true solutions of equations (14)–(17) is no longer valid. Large values of the neutral velocity correspond to large density changes, which will eventually lead to unphysical negative densities if the linear formulas are used for initial disturbances of increasing magnitude. (It is assumed that the magnitude of the initial disturbance is some increasing function of the energy which generates the initial disturbance.)

For a number of localized disturbances, which would individually generate velocity distributions such as equation (46), the velocity, in the linear approximation, would be given by the sum of the individual velocities, and the corresponding electron density would be calculated using this sum. If this number of initial disturbances becomes too large, however, then this sum will eventually approach, in magnitude, the speed of sound, leading to similar difficulties described in the previous paragraph.

To model a large number of localized disturbances of arbitrary magnitude, it is necessary to deal with these nonlinear issues. We will not be so ambitious as to try to approximate corrections to the actual equations of motion, but instead will tr to construct solutions with certain reasonable properties which will be stated below. The results of this section must, therefore, be looked upon in their proper light as, at best, educated guesses. The assumptions which will guide our approach to modeling large disturbances are:

1. The electron density must always be positive.
2. The solutions must approach the linear solutions for small initial disturbances.
3. The magnitude of the velocity must approach a constant as the altitude increases.

This last assumption is based on remarks stated in section 4.4 that in a realistic atmosphere gravity waves become damped with increasing altitude in such a way that the factor $\exp(z/2H)$ is almost exactly cancelled.

We will now outline the reasoning which will lead to a solution with the properties enumerated above. The vertical velocity of electrons, w_e, according to equation (68) is

$$w_e = (\mathbf{v} \cdot \hat{\mathbf{B}})(\hat{\mathbf{e}}_z \cdot \hat{\mathbf{B}}), \tag{77}$$

where the neutral velocity is $\mathbf{v} = u\hat{\mathbf{e}}_h$ (the vertical velocity component, $w\hat{\mathbf{e}}_z$, can be added; it falls with distance faster than u by a factor of $1/r$). Remarks following equation (57) show that asymptotically the spatial phase of this velocity is zero and, therefore, the spatial variation is mild except for the $\exp(z/2H)$ factor. According to third assumption above, this factor must approach one for altitudes above the F-region peak, which will be called z_c. We will therefore try to find some function, call it $g(z)$, with the property that $g \to 1$ as $z \to \infty$ and $g \sim \exp(z/2H)$ for $z \ll z_c$ and write

$$w_e = g(z)w_0, \tag{78}$$

where

$$w_0 = (\hat{\mathbf{e}}_h \cdot \hat{\mathbf{B}})(\hat{\mathbf{e}}_z \cdot \hat{\mathbf{B}})e^{-z/2H}u. \tag{79}$$

The function w_0 is a very mild function of position and can be considered a function of time only when integrated. A choice for $g(z)$ which meets the assumptions is

$$g(z) = \frac{e^{(z-z_c)/2H}}{1 + e^{(z-z_c)/2H}}. \tag{80}$$

Consider electrons initially located at height z_0 (we will suppress the horizontal dependence of the electron position; vertical motion is mainly responsible for density changes). The equation of motion for the height of these electrons at time t, $z = z(z_0, t)$, is

$$\frac{\partial z}{\partial t} = \frac{e^{(z-z_c)/2H}}{1+e^{(z-z_c)/2H}}\, w_0, \qquad z(z_0,0) = z_0. \tag{81}$$

The solution of this equation is given implicitly by

$$z' - e^{-z'} = z_0' - e^{-z_0'} + D', \tag{82}$$

where

$$z' = \frac{z-z_c}{2H}, \qquad z_0' = \frac{z_0 - z_c}{2H}, \qquad D' = \frac{D}{2H}, \tag{83}$$

and

$$D = \int_0^t w_0(z_0, t')\, dt'. \tag{84}$$

The solution of equation (82), call it $z(z_0,t)$, can be determined most readily by simple numerical means. The inverse solution, $z_0 = z_0(z,t)$ can be determined in the same way from equation (82), where, for consistency, z should replace z_0 in equation (84). The solutions given are not exact, but approach the exact solution as the dependence of w_0 on z decreases.

The density of electrons, initially at z_0, with density $n_0(z_0)$, are determined by dividing by the jacobian of the transformation, $z_0 \rightarrow z$,

$$n_e(z,t) = \frac{n_0(z_0)}{J(z_0,t)}, \tag{85}$$

where

$$J(z_0,t) = \frac{\partial z}{\partial z_0} = \frac{1+e^{z_0'}}{1+e^{z'}}. \tag{86}$$

Alternatively, the density can be written, using the jacobian of the inverse transformation,

$$n_e(z,t) = n_0(z_0)j(z,t), \tag{87}$$

where

$$j(z,t) = \frac{\partial z_0}{\partial z} = \frac{1+e^{z'}}{1+e^{z'_0}}. \tag{88}$$

It can be readily seen from these equations that the jacobians, and hence the densities, remain positive for all $-\infty < D < \infty$, as required by the first assumption. The construction also makes it clear that for small velocities, and, hence, small values of D, the solution approaches the linear solution given by equation (72), as demanded by the second assumption.

An extension for N localized disturbances can be obtained simply by summing the quantity D_i due to each localized disturbance individually, which will now be called D,

$$D = \sum_{i=1}^{N} D_i, \qquad i = 1, \ldots, N, \tag{89}$$

where

$$D_i = \int_0^t w_{0,i}(z,t')\,dt'. \tag{90}$$

and $w_{0,i}$ is vertical velocity of electrons produced by the ith localized disturbance (divided by g). One then solves equation (82) to find the initial position of electrons and equation (87) to compute the density. As for $N = 1$, all three of the required assumptions are met by this solution.

SECTION 6

OTHER MECHANISMS FOR CHANGE IN ELECTRON DENSITY

Thus far we have been concerned with changes in ionospheric electron density due only to volume changes produced by motion of the electrons driven by the passage of an acoustic-gravity wave. Electrons can be freed into the ionosphere by photoionization of atmospheric constituents, mainly nitrogen and oxygen (either molecular or atomic), by the sun (and other, less important, forms of radiation). The rate of electron production at a given location does not depend on the amount of electrons present, but rather on the intensity of the radiation and the amount of atmospheric gases present. Electrons can be absorbed (or freed) via photochemical and other reactions with atmospheric constituents, such as recombination and detachment. The rate of electron loss due to such reactions depends on the density of electrons present. It will not be necessary for what follows to describe the individual processes involved (see reference 7 for further details). In addition to production and loss mechanisms, electron density can also change through transport processes, such as diffusion. Our object in this section is to amend equation (87) of the previous section in a simple way which accounts for electron density changes due to these processes as modified by the passage of a gravity wave.

The basic strategy will be as follows: we will first show that loss mechanisms conspire with diffusion in such a way that the ionosphere, during nighttime, decays in a shape preserving manner, which leads to the first assumption that photochemical loss at all altitudes of interest depends on the chemical loss rate at the electron density peak. By assuming a single decay rate for the entire ionospheric profile still applies during the passage of a gravity wave, we will then derive a formula which gives the change in this rate as a function of the parameters describing the gravity wave. This formula will then be added to equation (87) in a reasonable manner. At this point, the reader should be reminded that not all results arrived at in this section will be rigorously derived from first principles, and the results should be viewed in the same spirit as the previous section.

According to the remarks made above, the continuity equation for electrons can be written

$$\frac{\partial n_e}{\partial t} + \nabla \cdot (n_e \mathbf{v}_e) = q - l, \tag{91}$$

where the electron density, n_e, and velocity, $\mathbf{v}_e$, and the electron production rate, q, are all functions of position and time. The electron loss rate, $l(\mathbf{r},t) = L(n_e(\mathbf{r},t),\mathbf{r},t)$, is also a function of position and time through its dependence of the function L on n_e. The electron velocity can be thought of as the sum of two velocities, one which occurs in ambient conditions due to transport and the other due to gravity wave induced electron motion. The electron production rate is usually assumed to be zero during the nighttime and a function of only altitude during the day (a consequence of a stratified atmosphere), with a mild time dependence due to the travel of the sun across the daytime sky. A useful form for the electron production rate as a function of altitude is the classical Chapman formula, which can be written

$$q = q_m \exp\left[1 - \frac{z - z_c}{H} - \sec\chi\, e^{-(z-z_c)/H}\right], \tag{92}$$

where χ is the solar zenith angle, and q_m is the production rate at the altitude of the electron density peak, z_c, for vertical solar radiation, $\chi = 0$. This form for q is derived under the assumption the that atmosphere is made up of a single absorbing gas whose density decreases exponentially with altitude with constant scale height, H, (see reference 7).

For electrons at F-region heights and above, to quite a good approximation, the electron density loss rate is proportional to the electron density, with the proportionality constant a function of altitude only, dependent on the concentration of neutral atomic constituents. As shown in reference 7, the loss rate can be written

$$l = \beta n_e, \qquad \beta = \beta_0 e^{-\gamma(z-z_c)/H}, \tag{93}$$

where β_0 is loss rate at altitude z_c. The constant, γ, depends on the relative scale heights of the ionizable gas and linear loss coefficient and is equal to about 1.75 for altitudes above the E region. If there were no transport processes it can be seen that electrons would be lost at low altitudes at exponentially increasing rates, which is not the case.

6.1 DIFFUSION.

We will now show how electron diffusion can be derived from the equations of motion in the simplest possible case and how, under the assumption that the electron loss rate is given by equation (93), this diffusion controls the decay of

the ionospheric profile in such a way that its shape of the profile is preserved. We assume the ionosphere can be described by a two component charged fluid made of ions and electrons undergoing collisions with themselves and a neutral background. The equations of motion are then

$$m_i \frac{D\mathbf{v}_i}{Dt} = m_i\mathbf{g} - \frac{1}{n_i}\nabla(n_i k T_i) + e(\mathbf{E} + \mathbf{v}_i \times \mathbf{B}) - m_i\nu_{in}(\mathbf{v}_i - \mathbf{v}_n) - m_e\nu_{ei}(\mathbf{v}_i - \mathbf{v}_e), \quad (94)$$

$$m_e \frac{D\mathbf{v}_e}{Dt} = m_e\mathbf{g} - \frac{1}{n_e}\nabla(n_e k T_e) - e(\mathbf{E} + \mathbf{v}_e \times \mathbf{B}) - m_e\nu_{en}(\mathbf{v}_e - \mathbf{v}_n) - m_e\nu_{ei}(\mathbf{v}_e - \mathbf{v}_i), \quad (95)$$

where for electrons m_e is the mass, n_e the density, $\mathbf{v}_e$ the velocity, and T_e the temperature, and similarly for ions, ν_{in} is the collision rate between ions and neutrals, ν_{en} the collision rate between electrons and neutrals, and ν_{ei} the collision rate between electrons and ions, $\mathbf{E}$ is the electric field, $\mathbf{B}$ the magnetic field, $\mathbf{g}$ the acceleration due to gravity, k is Boltzmann's constant, and $\mathbf{v}_n$ is the neutral velocity.

The simplest case is time-independent vertical diffusion in a vertical magnetic field. In this case the equations of motion reduce to (all quantities depend only on the vertical coordinate, z)

$$\frac{d(n_i k T_i)}{dz} = -n_i m_i g + n_i e E - n_i m_i \nu_{in}(w_i - w_n), \quad (96)$$

$$\frac{d(n_e k T_e)}{dz} = -n_e m_e g - n_e e E - n_e m_e \nu_{en}(w_e - w_n). \quad (97)$$

Under the further simplifying assumptions that $m_i \gg m_e$, $n_i = n_e = n$, $w_i = w_e = w_d$ (plasma drift velocity), $w_n = 0$, and $m_i\nu_{in} \gg m_e\nu_{en}$, addition of the two equations gives for the plasma drift velocity

$$w_d = -\frac{1}{m_i\nu_{in}}\left(\frac{1}{n}\frac{d}{dz}\left[nk(T_i + T_e)\right] + n_i m_i g\right). \quad (98)$$

With the further definitions

$$T_p = \frac{1}{2}(T_i + T_e) \qquad , \qquad H_p = \frac{2kT_p}{m_i g}, \tag{99}$$

the plasma drift velocity becomes

$$w_d = -D\left(\frac{1}{n}\frac{dn}{dz} + \frac{1}{T_p}\frac{dT_p}{dz} + \frac{1}{H_p}\right), \tag{100}$$

where the plasma diffusion coefficient, D, is

$$D \equiv \frac{2kT_p}{m_i \nu_{in}}. \tag{101}$$

Simplifying further, we assume the ion mass and neutral mass are equal and are distributed with scale height, H, and that $T_i = T_e = T$, which gives

$$D = D_0 e^{(z-z_c)/H}, \tag{102}$$

where D_0 is the diffusion coefficient at z_c. The plasma drift velocity is finally given by

$$w_d = -D_0 e^{(z-z_c)/H}\left(\frac{1}{n}\frac{dn}{dz} + \frac{1}{2H}\right). \tag{103}$$

Notice that the diffusion coefficient increases exponentially with altitude, while the electron loss rate, β, given in equation (93), decreases exponentially with altitude. It is expected that the effects will counteract one another is such a way that a peak electron density will occur near where β and D/H^2 are equal. This analysis can be generalized by removing some of the simplifying assumptions used in this derivation (such as including an inclined magnetic field and a nonzero neutral wind).

We will now try to find solutions of the continuity equation (91), assuming a loss term given by equation (93) and an electron velocity given by equation (103). Assuming vertical motion only and taking $q = 0$ for simplicity, equation (91) becomes

$$\frac{\partial n_e}{\partial t} = -\beta n_e - \frac{\partial}{\partial z}(n_e w_d), \tag{104}$$

where n_e is now considered a function of z and t. Assuming a solution of the form

$$n_e(z,t) = \eta(z)e^{-\lambda t}, \tag{105}$$

and using equation (103) gives

$$-\frac{d}{dz}\left[D\left(\frac{d\eta}{dz}+\frac{\eta}{2H}\right)\right]+\beta\eta = \lambda v. \tag{106}$$

This equation can be made into an eigenvalue problem for λ by supplementing it with appropriate boundary conditions. We assume that the electron density is zero at the ground and falls off rapidly enough as $z \to \infty$ to insure a denumerable number of eigenvalues. Making the substitution

$$\eta = e^{-(z-z_c)/2H}\mu, \tag{107}$$

puts equation (106) in standard Sturm-Liouville form

$$-\frac{d}{dz}\left[p\frac{d\mu}{dz}\right]+q\mu = \lambda r\mu, \tag{108}$$

with boundary conditions, say,

$$\mu(0) = 0, \qquad \lim_{z\to\infty}\frac{d\mu}{dz} = 0, \tag{109}$$

and where

$$p(z) = D(z)e^{-(z-z_c)/2H}, \qquad q(z) = \beta(z)e^{-(z-z_c)/2H}, \qquad r(z) = e^{-(z-z_c)/2H}. \tag{110}$$

It is well known that nontrivial solutions to equation (108) exist for a denumerable number of real eigenvalues, λ_n. Multiplying equation (108) by μ, then integrating from 0 to ∞, and using the boundary conditions (109) shows that

$$\lambda = \frac{\int_0^\infty \left[p\left(\frac{d\mu}{dz}\right)^2 + q\mu^2 \right] dz}{\int_0^\infty r\mu^2 \, dz} > 0, \tag{111}$$

which follows from equations (110), (93), and (102), where it is obvious that p, q, and r are positive. Therefore, all eigenvalues are greater than zero. The general solution to equation (104) can be written as a sum of terms of the form (105) with all terms, and therefore, n_e, decaying in time. Furthermore, eventually the term with the smallest eigenvalue, λ_0, will dominate the sum and the solution will rapidly approach the shape preserving form

$$n_e(z,t) = n_0(z)e^{-\lambda_0 t}, \tag{112}$$

It can further be shown (see reference 7 and references contained therein) that the peak of the function n_0 occurs near where $\beta = D/H^2$, which we have denoted β_0, and that the smallest decay rate is approximately equal to the electron loss rate at the altitude of the peak, i.e. $\lambda_0 = \beta_0$. It can also be shown that during the daytime, $q \neq 0$, an equilibrium solution can be found such that the electron peak occurs at approximately the same altitude and that the peak electron density, $n_m = n_0(z_c)$, is approximately equal to β_0/q_0, where q_0 is the value of the solar production rate at the altitude of the peak, which by equation (92) is $q_0 = q_m \exp(1 - \sec\chi)$ for a Chapman layer.

6.2 CHANGE IN LOSS RATE DUE TO GRAVITY WAVES.

We have seen above that in the absence of gravity waves an ionospheric profile approximately keeps its shape and decays (in the absence of solar radiation) with a rate approximately equal to the electron loss rate at the altitude of the electron density peak. In the presence of solar radiation the peak approaches a constant value approximately equal to β_0/q_0, with transient terms decaying with a rate approximately equal to β_0. We now assume that during and following the passage of one or more gravity waves, the electron density profile is changed due to hydrodynamic motions described earlier, but in addition, the electron density returns to its ambient state in such a way that the induced transient terms decay with a single rate for the entire profile, which is given by the ambient rate plus a correction term which depends on

parameters describing the gravity wave. We will now compute an approximation for this correction term.

Let the density of electrons at the peak be denoted n_m, and let the motion of the electrons in the peak induced by the gravity waves be $z(t)$, with $z(0) = z_c$. The continuity equation gives for these electrons

$$\frac{dn_m}{dt} = -\beta n_m + Q - \frac{d}{dt}(\log J), \tag{113}$$

where all quantities in this equation are functions of time only, that is,

$$\beta(t) = \beta_0 e^{-\gamma(z(t)-z_c)/H}, \tag{114}$$

$$Q(t) = q(z(t)), \tag{115}$$

with $q(z)$ given by equation (92), and

$$J(t) = \frac{\partial z}{\partial z_0}(z_c, t). \tag{116}$$

It will be assumed that J is given by equation (86), i.e. no other electron motion of the peak is induced by the passage of the gravity wave other than the direct coupling to the neutral motion given by equation (77).

The solution of equation (113) is readily determined,

$$n_m = \frac{e^{-K(t)}}{J(t)}\left[\int_0^t e^{K(t')} J(t') Q(t')\, dt' + n_{m,0}\right], \tag{117}$$

where

$$K(t) = \int_0^t \beta(t')\, dt', \tag{118}$$

and $n_{m,0} = n_m(0)$, the electron density at the peak immediately following the passage of the gravity waves, which is taken as $t = 0$.

For no gravity wave motion, $z(t) = z_c$, $J(t) = 1$, the solution (117) becomes

$$n_m = \left(n_{m,0} - \frac{q_0}{\beta_0} \right) e^{-\beta_0 t} + \frac{q_0}{\beta_0}. \tag{119}$$

It is clear from this equation that if the initial electron density, $n_{m,0}$, is not equal to the equilibrium value, q_0/β_0, then the solution will approach the equilibrium value with the transient terms decaying with a rate equal to β_0.

Evaluation of the integrals appearing in equations (117) and (118) for arbitrary motion can be performed in a straightforward manner by numerical means, however, this would not suit the purposes of a model. We therefore seek an approximate solution, which can readily be compared with exact evaluation of the integrals. The sought after approximate solution will be determined in stages, by considering increasingly general cases.

First consider an undamped gravity wave motion in the absence of solar radiation, given by $z(t) = z_c + a \sin \omega t$, $J(t) = 1$, $Q(t) = 0$. The solution (117) becomes

$$n_m = n_{m,0}\, e^{-K(t)}, \qquad K(t) = \beta_0 I(t), \tag{120}$$

where

$$I(t) = \int_0^t e^{-b \sin \omega t'}\, dt', \tag{121}$$

and $b = \gamma a$. It can easily be shown that

$$I(t) = I_0(b)(t - \tau) + \text{oscillatory terms}, \qquad 0 \leq \omega\tau \leq 2\pi, \tag{122}$$

where I_0 is the zeroth order modified Bessel function of the first kind. For small b, the power series expansion of I_0 gives,

$$I(t) \sim \left(1 + \frac{b^2}{4} \right) t, \tag{123}$$

so that the solution (120) becomes

$$n_m = n_{m,0}\, e^{-\beta t}, \qquad \beta = \beta_0 \left(1 + \frac{b^2}{4}\right), \tag{124}$$

Notice that for a single undamped gravity wave with amplitude not too large, the peak electron density decays with a rate equal to the ambient rate plus a second order correction that depends only on the amplitude of the wave and not on the frequency. There is no first order correction, which shows that the amplitude must be somewhat large to see a change in decay rate.

An alternative way of calculating the correction to the decay rate is to expand the integrand in equation (121)

$$I(t) = \int_0^t \sum_{n=0}^{\infty} (-b \sin \omega t')^n \, dt'. \tag{125}$$

Retaining terms to second order gives

$$I(t) = \left(1 + \frac{b^2}{4}\right) t + \frac{b}{\omega} \cos \omega t \left(1 - \frac{b}{4} \sin \omega t\right) - \frac{b}{\omega} + \cdots, \tag{126}$$

which gives the same second order change in the decay rate as in equation (123).

We now generalize this result by considering a damped gravity wave, such that $z(t) = z_e + ae^{-\lambda t} \sin \omega t$, $J(t) = 1$, $Q(t) = 0$. The solution is again given by equation (120) with

$$I(t) = \int_0^t \exp\left[-be^{-\lambda t'} \sin \omega t'\right] dt', \tag{127}$$

Expanding in the same way as equation (125) gives

$$I(t) = t + \frac{b^2}{8\lambda} \frac{\omega^2}{\lambda^2 + \omega^2} \left(1 - e^{-2\lambda t}\right) + \cdots. \tag{128}$$

Notice that this gives the same result as in equation (126) in the limit as $\lambda \to 0$. This solution gives a decay rate which initially has a second order increase, but eventually returns to its ambient value, as would be expected as the gravity wave damps out.

Generalizing further let the electron motion be given by the sum of N damped gravity waves with differing frequencies and phases,

$$z(t) = z_c + \sum_{i=1}^{N} a_i e^{-\lambda_i t} \sin(\omega_i t + \phi_i), \qquad i = 1, \ldots, N. \tag{129}$$

The solution is

$$I(t) = \int_0^t \exp\left[-\sum_{i=1}^{N} a_i e^{-\lambda_i t'} \sin(\omega_i t' + \phi_i)\right] dt', \tag{130}$$

With a bit more algebra one can show that to second order, for $\omega_i \neq \omega_j$, $i \neq j$,

$$I(t) = t + \frac{1}{8} \sum_{i=1}^{N} \frac{b_i^2}{\lambda_i} \frac{\omega_i^2}{\lambda_i^2 + \omega_i^2} \left(1 - e^{-2\lambda_i t}\right) + \cdots. \tag{131}$$

Most interesting about this result is that if the frequencies of oscillation are different, then the second order correction is given by the sum of terms which apply for one oscillation (as in equation (128)), there is no mixing of terms (no terms in $b_i b_j$, $i \neq j$).

If the gravity wave is damped using a gaussian, as was chosen in equation (74),

$$z(t) = z_c + \sum_{i=1}^{N} a_i e^{-\lambda_i^2 t^2} \sin(\omega_i t + \phi_i), \qquad i = 1, \ldots, N, \tag{132}$$

then, assuming $\lambda_i \ll \omega_i$,

$$I(t) = t + \frac{1}{8} \sum_{i=1}^{N} \frac{b_i^2}{\lambda_i^2 t} \left(1 - e^{-2\lambda_i^2 t^2}\right) + \cdots. \tag{133}$$

This is the most general form we will use for the change in the decay rate due to the presence of many damped gravity waves.

Performing the more general calculations when $Q(t) \neq 0$ and $J(t) \neq 1$ becomes prohibitively more difficult. It turns out that to the order in which we are working we can approximate the solution (117), by

$$n_m = \left[\left(n_{m,0} - \frac{q_0}{\beta(t)}\right) e^{-\beta(t)t} + \frac{q_0}{\beta(t)}\right] \Big/ J(t), \tag{134}$$

where

$$\beta(t) = \beta_0 I(t)/t. \tag{135}$$

A comparison of the approximate formula (134) with the exact result (117), is shown in figure 7. The electron density has been converted to critical frequency using equation (1) for a case similar to that shown in figure 1. As can be seen, the approximate result (dashed line), agrees well with the exact integral (solid line).

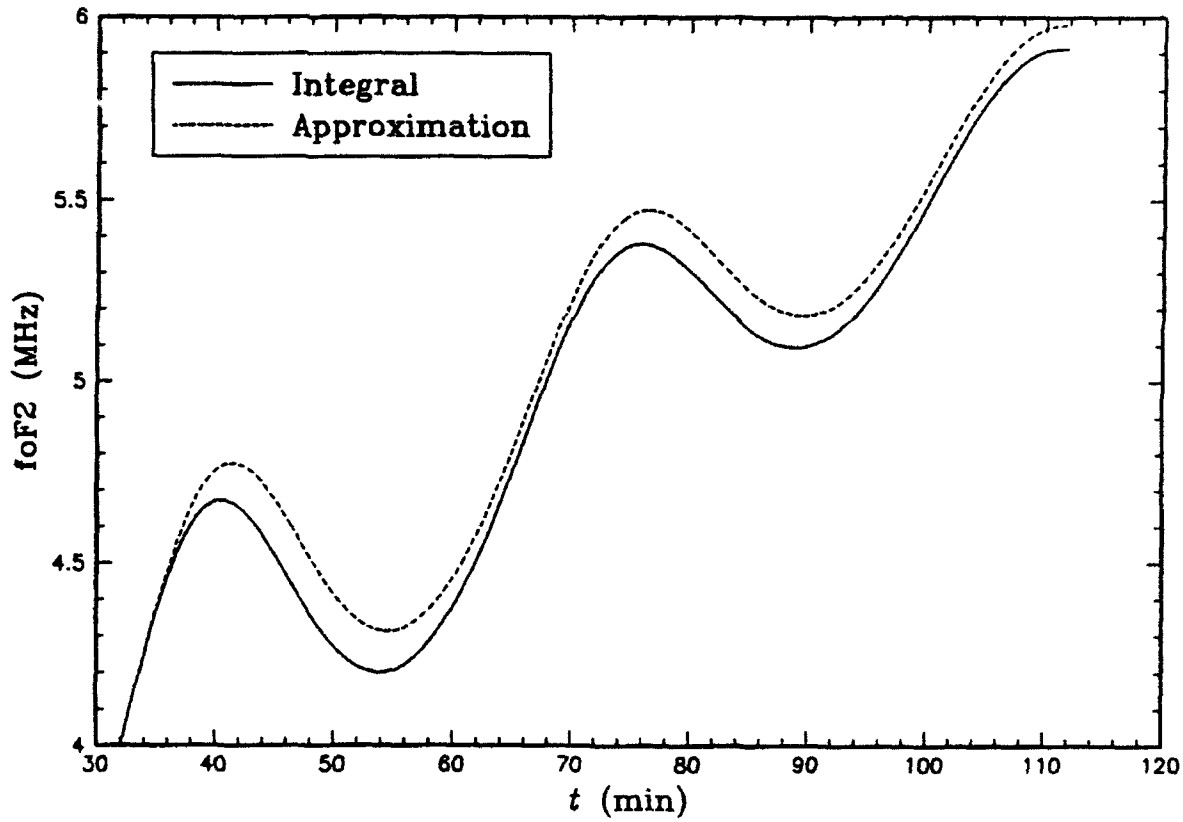

Figure 7. **A comparison of critical frequency vs. time using the approximate formula (134) with exact integral (117).**

SECTION 7

THE MODEL

We will now assemble all of the ideas derived in the previous sections into a working model. It will be necessary for both consistency and simplicity to make some changes in the formulas presented earlier, as well as to include features not previously discussed. All the derivations were carried out in cartesian coordinates, assuming a flat earth, with an atmosphere of constant temperature and, therefore, constant scale height and speed of sound. The model must compute electron densities above a round earth, so the necessary geometrical changes will be made. The actual atmosphere has a scale height which increases with altitude. For simplicity, we will choose an average scale height and speed of sound, which give results that best approximate the data. In section 4.4 it was shown that the amplitude of gravity wave-induced ionospheric disturbance falls off as the inverse distance from the source under the assumptions made in that section. In a more realistic case, there will be other mechanisms which will cause damping of the wave. We will add an exponential damping term to account for this expected behavior, with the length scale chosen to best agree with the data.

The ambient electron density profile for the ionosphere in general depends on location and time of day (as well as other factors such as season, solar activity, etc.). For modeling purposes we will use two vertically-stratified electron density profiles to represent typical day and nighttime cases. The altitude of the electron density peak, z_e, will be taken to be 300 km and the ambient electron loss rate at this altitude, β_0, will be chosen to reproduce typical nighttime behavior. The daytime electron production rate q_0 will be chosen such that $n_0 = q_0/\beta_0$, where n_0 is daytime electron density profile.

7.1 CONSTANTS AND AUXILIARY FUNCTIONS.

The following list of constants have been chosen to best fit the available data (they may be changed by the user):

$$c = .7 \text{ km/sec}, \qquad z_e = 300 \text{ km}, \qquad H = 40 \text{ km}, \tag{136}$$

$$x_0 = 1 \times 10^4 \text{ km}, \qquad A_0 = 50 \text{ km/MT}, \qquad m_0 = .45 \text{ MT}^{-1/2}, \tag{137}$$

$$\beta_0 = 1 \times 10^{-4} \text{ sec}^{-1}, \qquad \gamma = 1.75. \tag{138}$$

It is assumed that the model is provided with a number of external functions which can be called when necessary. They are:

Electron density profile: $n_0(z)$ (one for day and one for night),

Brunt-Väisälä frequency: $\omega_b(z)$,

Acoustic cutoff frequency: $\omega_a(z)$,

A function: $z_0(z, D)$ and its inverse $z(z_0, D)$, which are solutions of

$$z' - e^{-z'} = z_0' - e^{-z_0'} + D', \tag{139}$$

where

$$z' = \frac{z - z_c}{H}, \qquad z_0' = \frac{z_0 - z_c}{H}, \qquad D' = \frac{D}{H}. \tag{140}$$

7.2 INPUTS AND OUTPUTS.

The earth is taken to be a sphere of radius R_e, with a spherical coordinate system, (r, θ, ϕ), centered at the center of the sphere. The earth's magnetic field is taken to be a magnetic dipole with axis along the polar axis of the spherical coordinate system.

The inputs to the model are the locations, yields, and times of burst of N explosions, and the location and time at which the electron density is desired (observation point). The following list describes each input parameter:

θ_i, $i = 1, \ldots, N$: colatitude of the ith burst,

ϕ_i, $i = 1, \ldots, N$: longitude of the ith burst,

$z_{b,i}$, $i = 1, \ldots, N$: altitude of the ith burst in km,

Y_i, $i = 1, \ldots, N$: yield of the ith burst in MT,

$t_{0,i}$, $i = 1, \ldots, N$: time of the ith burst in seconds,

θ: colatitude of the observation point,

ϕ: longitude of the observation point,

z: altitude of the observation point,

t: time of observation.

The outputs of the model are the electron density as a function of position and time,

$$n_e(r, \theta, \phi, t),$$

each partial derivative of n_e with respect to r, θ, ϕ, and t,

$$\frac{\partial n_e}{\partial r}, \qquad \frac{\partial n_e}{\partial \theta}, \qquad \frac{\partial n_e}{\partial \phi}, \qquad \frac{\partial n_e}{\partial t},$$

as well as all second order partial derivatives of n_e with respect to r, θ, and ϕ,

$$\frac{\partial^2 n_e}{\partial r^2}, \quad \frac{\partial^2 n_e}{\partial \theta^2}, \quad \frac{\partial^2 n_e}{\partial \phi^2}, \quad \frac{\partial^2 n_e}{\partial r \partial \theta}, \quad \frac{\partial^2 n_e}{\partial r \phi}, \quad \frac{\partial^2 n_e}{\partial \theta \partial \phi}.$$

We will only present the formulas for the electron density, n_e, the formulas for the first and second partial derivatives can be obtained from these formulas by a straightforward, though tedious, application of the chain rule of the differential calculus of many variables.

7.3 MODEL ALGORITHM.

The electron density, $n_e(z, \theta, \phi, t)$, is computed as follows:

$$r_{b,i} = R_e + z_{b,i}, \qquad i = 1, \ldots, N, \tag{141}$$

$$z_i = z - z_{b,i}, \tag{142}$$

$$\cos\theta_{z,i} = \cos\theta\cos\theta_i + \sin\theta\sin\theta_i\cos(\phi - \phi_i), \tag{143}$$

$$x_i = r_{b,i}\theta_{z,i}, \tag{144}$$

$$R_i^2 = x_i^2 + z_i^2, \tag{145}$$

$$\sin\lambda = \frac{2\cos\theta}{(1 + 3\cos^2\theta)^{1/2}}, \tag{146}$$

$$\cos\alpha_i = \frac{\cos\theta_i - \cos\theta\cos\theta_{z,i}}{\sin\theta\sin\theta_{z,i}}, \tag{147}$$

$$P_i = \frac{1}{2}\left(\cos\alpha_i \sin 2\lambda \frac{x_i}{R_i} - 2\sin^2\lambda\frac{z_i}{R_i}\right), \tag{148}$$

$$E_i = e^{-z_i/z_0}, \tag{149}$$

$$t_{1,i} = \frac{R_i}{c}\frac{\omega_a(z)}{\omega_b(z)} + t_{0,i}, \tag{150}$$

$$\omega_i = \omega_b(z)\frac{z_i}{R_i}\left(1 + \frac{1}{2}\frac{\omega_a^2(z)}{\omega_b^2(z)}\frac{R_i^2}{c^2(t - t_{0,i})^2}\right), \tag{151}$$

$$Q_i = \sin\left(\omega_i(t - t_{1,i})\right), \tag{152}$$

$$A_i = A_0 Y_i, \qquad m_i = m_0\sqrt{Y_i}, \tag{153}$$

$$a_i = \frac{2\pi m_i}{z_i}, \tag{154}$$

$$k_i = \omega_b(z)(t - t_{1,i})\frac{R_i}{x_i^2}, \tag{155}$$

$$S_i = A_i \exp\left(-k_i^2/a_i^2\right), \tag{156}$$

$$D_i = S_i Q_i E_i P_i, \tag{157}$$

$$D = \sum_{i=1}^{N} D_i, \tag{158}$$

$$d_i = A_i E_i P_i, \tag{159}$$

$$\lambda_i = \frac{\omega_b(z_c)}{2\pi m_i}\frac{z_c - z_{b,i}}{x_i}, \tag{160}$$

$$b^2 = \sum_{i=1}^{N} \frac{d_i^2}{8\lambda_i^2(t - t_{1,i})^2}\left(1 - e^{-2\lambda_i^2(t-t_{1,i})^2}\right), \tag{161}$$

$$b = +\sqrt{b^2}, \tag{162}$$

$$\beta = \beta_0\left[1 + \left(\frac{\gamma}{H}\left[z(z_c, -b) - z_c\right]\right)^2\right], \tag{163}$$

$$q_0 = \begin{cases} \beta_0 n_0(z), & \text{day} \\ 0, & \text{night} \end{cases}, \tag{164}$$

$$z_0 = z_0(z, D), \tag{165}$$

$$J = \frac{1 + e^{-z_0'}}{1 + e^{-z'}}, \tag{166}$$

$$\hat{t} = t - \min_i(t_{1,i}), \tag{167}$$

$$n_e = \left[\left(n_0(z_0) - \frac{q_0}{\beta}\right) e^{-\beta \hat{t}} + \frac{q_0}{\beta}\right] \Big/ J. \tag{168}$$

7.4 RESULTS.

Figures 8 and 9 are electron density (plasma frequency) contour plots generated using the AGW model. For each plot, the electron density following the detonation of four simultaneous high-yield, near surface bursts at two hours is plotted for the surrounding region. Figure 8 is the daytime case and figure 9 is the nighttime case.

The lower portions of each figure are electron density contours in a horizontal plane 300 km above the earth's surface. The distance between the tick marks is 556 km. The upper portions of each figure are electron density contours in a vertical plane which intersects the lower portion of the figure along the line shown in the center of the figure. It is clear from the figures that the effect of the gravity waves is to distort the normally vertically stratified ionosphere into regions of varying density on scales of about 10 km to 100 km. Notice that the effect is more prominent during nighttime. During the daytime, the sun acts to more swiftly return the ionosphere to its ambient state. Further details concerning these plots, as well as the implementation and use of the AGW model in the RAYTRACE code and its subsequent application for an HF signal specification can be found in the companion report, reference 6.æ

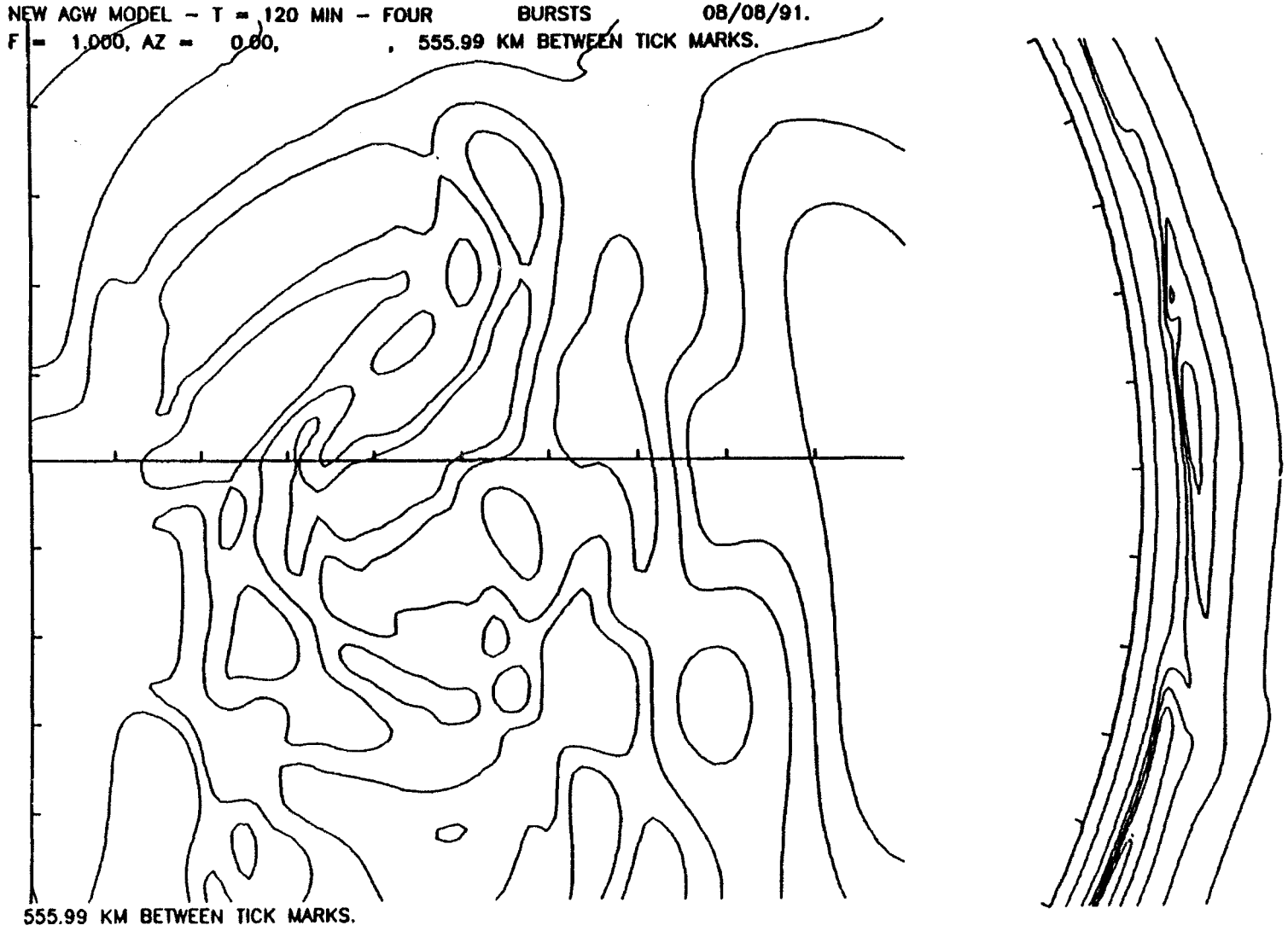

Figure 8. Electron density contour plots at two hours following the detonation of four high-yield, near-surface bursts, during daytime.

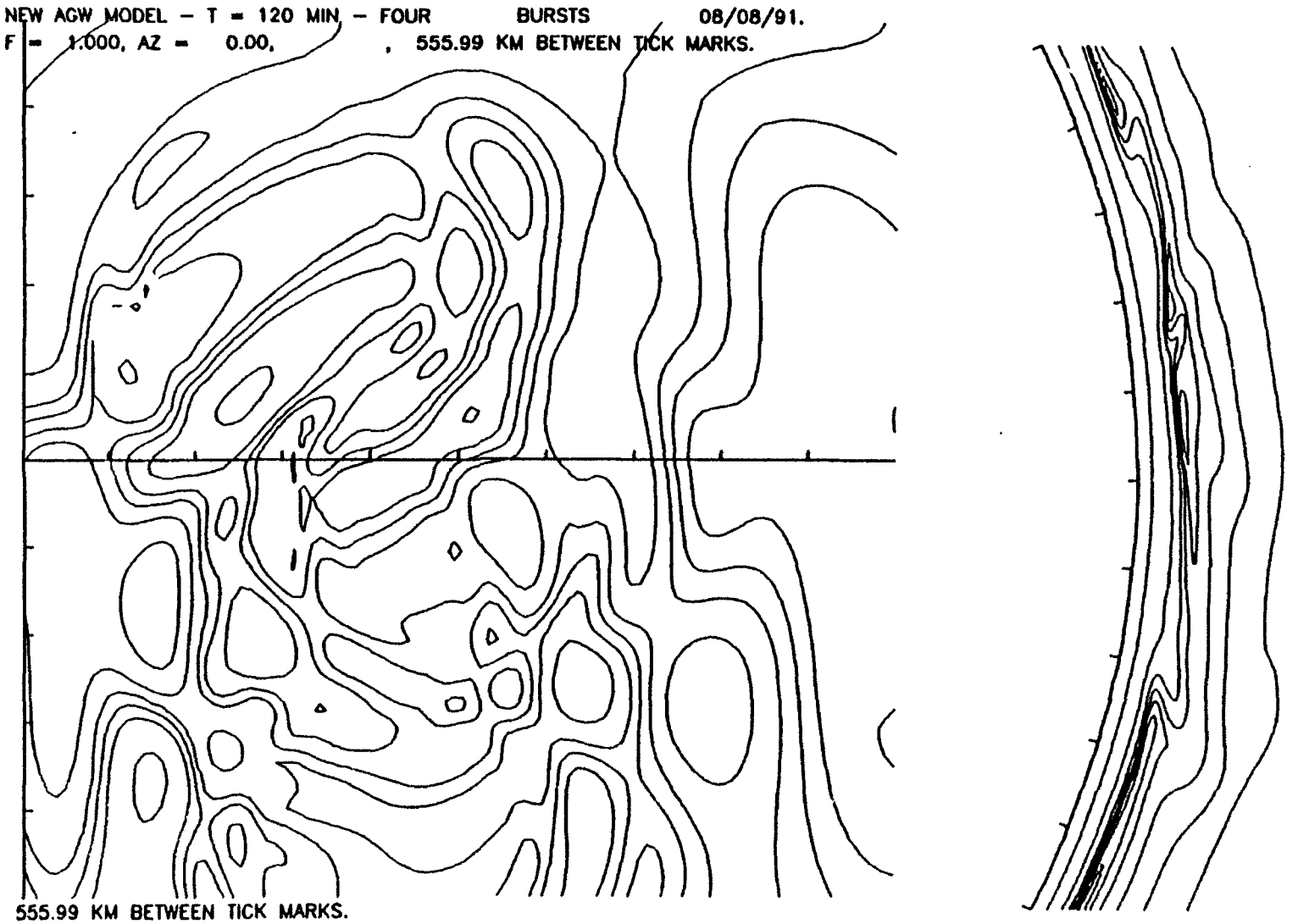

Figure 9. Electron density contour plots at two hours following the detonation of four high-yield, near-surface bursts, during nighttime.

SECTION 8

LIST OF REFERENCES

1. Bleistein, N. and R. A. Handelsman, (U) *Asymptotic Expansions of Integrals*, Holt, Rinehart and Winston, New York, 1975. (U)

2. Hines, C. O., (U) *Internal Atmospheric Gravity Waves at Ionospheric Heights*, Canadian Journal of Physics, **38**, pages 1441–1481, 1960. (U)

3. Hooke, W. H., (U) *Ionospheric Irregularities Produced by Internal Atmospheric Gravity Waves*, Journal of Atmospheric and Terrestrial Physics, **30**, pages 795–823, 1967. (U)

4. Kanellakos, D., (U) *Response of the Ionosphere to the Passage of Acoustic-Gravity Waves Generated by Low-Altitude Nuclear Explosions*, Journal of Geophysical Research, Volume 72, No. 17, pages 4559–4576, September 1967. (U)

5. Klostermeyer, J., (U) *Influence of Viscosity, Thermal Conduction, and Ion Drag on the Propagation of Atmospheric Gravity Waves in the Thermosphere*, Zeitschrift für Geophysik, **38**, pages 881–890, 1972. (U)

6. Nickisch, L. J., (U) *HF Signal Specification: Methodology Report*, 1992. (U)

7. Rishbeth, H. and O. K. Garriott, (U) *Introduction to Ionospheric Physics*, Academic Press, New York, 1969. (U)

8. Yeh, K. C. and C. H. Liu, (U) *Theory of Ionospheric Waves*, Academic Press, New York and London, 1972. (U)

9. Yeh, K. C., C. H. Liu and M. Y. Youakim, (U) *Attenuation of Internal Gravity Waves in Model Atmospheres*, Annals of Geophysics, **31**, pages 321–328, 1975. (U)

SECTION 9

GLOSSARY OF SYMBOLS

a	$2\pi m/z$ and AGW amplitude
b	γ a
$\hat{B}$	earth's magnetic field
c	speed of light, or sound
c_v	specific heat (constant volume)
$\tilde{c}$	(ω_b/ω_a) c
D	plasma diffusion constant
D_0	plasma diffusion constant (reference)
f	wave frequency
foF2	critical frequency of F_2 layer
f_p	plasma frequency
f(r)	initial velocity distribution
$\tilde{f}$(k)	fourier transform of f(r)
g	acceleration of gravity
g(z)	height function
h	true height
H	scale height
h'	virtue height
I(λ)	stationary phase integral
j	inverse jacobian
J	jacobian
k	wave number
K	constant
k_i	ith component of k
k_h	horizontal wave number
k_o	stationary phase solution
ℓ	electron loss term
m	number of cycles
m_e	electron mass
m_i	ion mass
m_o	number of cycles at yield one
n	index of refraction
N	number of disturbances
n'	perturbation in electron density
n_e(z)	electron density at height z
$n_{e,max}$	ionospheric peak electron density
n_i	ion number density
n_m	electron density at peak
$n_{m,\phi}$	electron density at peak just after AGW
n_ϕ	ambient electron density
p	pressure
$p^{(i)}$	ith pressure perturbation
p_0	pressure at height zero
q	electron production rate
q_ϕ	electron production rate at peak
r	radius
R_e	earth's radius
r_h	cylindrical radius
s	entropy
t	time
T_e	electron temperature
T_i	ion temperature
T_p	plasma temperature
T_ϕ	disturbance onset time
u	horizontal speed
U	constant
$u^{(i)}$	ith horizontal speed perturbation
u_x	$\partial u/\partial x$ (etc...)
U_o	U at Y 1
v	velocity
v_e	electron velocity
v_g	group velocity
v_i	ion velocity
$v^{(i)}$	ith vertical speed perturbation
w	vertical speed
W_d	plasma drift velocity
x	horizontal position
Y	yield
z	height

z'	scaled height
z_c	reference height
β	ℓ/n_e
β_ϕ	loss rate reference
γ	ratio of specific heats
$\eta(z)$	functional form of $n_e(z)$
θ	angle w.r.t. vertical
ϵ	expansion parameter
λ_n	eigenvalues of λ
λ_o	dominant eigenvalue
λ	parameter
$\mu(z)$	normalized functional form
ν_{in}	ion neutral collision frequency
ρ	density
ρ_0	density at height zero
$\rho^{(i)}$	ith density perturbation
χ	zenith angle
τ	ct/r
ω_e	vertical velocity of electrons
ω_b	Brunt-Väisälä frequency
ω_a	acoustic cutoff frequency
ω	angular frequency
ω_o	stationary phase frequency
ω_c	$\omega_b \cos\theta$

DISTRIBUTION LIST

DNA-TR-92-140

DEPARTMENT OF DEFENSE

ASSISTANT TO THE SECRETARY OF DEFENSE
ATTN: EXECUTIVE ASSISTANT

DEFENSE ADVANCED RSCH PROJ AGENCY
ATTN: CHIEF SCIENTIST

DEFENSE COMMUNICATIONS ENGINEER CENTER
ATTN: CODE R430 BOEHM

DEFENSE INFORMATION SYSTEMS
ATTN: SSS

DEFENSE NUCLEAR AGENCY
ATTN: NASC
ATTN: RAAE
ATTN: RAAE K SCHWARTZ
ATTN: RAAE R COX
ATTN: RAAE T BAZZOLI
2 CY ATTN: TITL

DEFENSE TECHNICAL INFORMATION CENTER
2 CY ATTN: DTIC/FDAB

FIELD COMMAND DEFENSE NUCLEAR AGENCY
ATTN: FCNM
ATTN: FCPRA LC R HEDTKE

U S NUCLEAR CMD & CENTRAL SYS SUPPORT STAFF
ATTN: SAB H SEQUINE

DEPARTMENT OF THE ARMY

U S ARMY ATMOSPHERIC SCIENCES LAB
ATTN: SLCAS-AE DR NILES

U S ARMY NUCLEAR & CHEMICAL AGENCY
ATTN: MONA-NU DR D BASH

U S ARMY NUCLEAR EFFECTS LABORATORY
ATTN: ATAA-PL
ATTN: ATAA-TDC
ATTN: ATRC-WCC LUIS DOMINGUEZ

U S ARMY SPACE & STRATEGIC DEFENSE CMD
ATTN: CSSD-TD W O DAVIES

U S ARMY STRATEGIC SPACE & DEFENSE CMD
ATTN: CSSD-SA

USA SURVIVABILITY MANAGMENT OFFICE
ATTN: SLCSM-SE J BRAND

DEPARTMENT OF THE NAVY

NAVAL OCEAN SYSTEMS CENTER
ATTN: CODE 542 J FERGUSON

NAVAL RESEARCH LABORATORY
ATTN: CODE 4700 S OSSAKOW

OFFICE OF NAVAL RESEARCH
ATTN: CODE 1114SP R G JOINER

DEPARTMENT OF THE AIR FORCE

AIR FORCE CTR FOR STUDIES & ANALYSIS
ATTN: AFSAA/SAKI

AIR FORCE ELECTRONIC WARFARE CENTER
ATTN: LT M MCNEELY
ATTN: SAVC
ATTN: SAZ

AIR UNIVERSITY LIBRARY
ATTN: AUL-LSE

DEPARTMENT OF ENERGY

LOS ALAMOS NATIONAL LABORATORY
ATTN: R W WHITAKER

SANDIA NATIONAL LABORATORIES
ATTN: TECH LIB 3141

DEPARTMENT OF DEFENSE CONTRACTORS

BERKELEY RSCH ASSOCIATES, INC
ATTN: J WORKMAN
ATTN: S BRECHT

JAYCOR
ATTN: J SPERLING

KAMAN SCIENCES CORP
ATTN: DASIAC

KAMAN SCIENCES CORPORATION
ATTN: B GAMBILL
ATTN: DASIAC
ATTN: R RUTHERFORD

LOCKHEED MISSILES & SPACE CO, INC
ATTN: R SEARS

LOGICON R & D ASSOCIATES
ATTN: E HOYT

MISSION RESEARCH CORP
2 CY ATTN: S BOTTONE

MISSION RESEARCH CORP
ATTN: W WHITE

MISSION RESEARCH CORP
ATTN: DAVE GUICE

MISSION RESEARCH CORP
ATTN: B R MILNER
ATTN: D KNEPP
ATTN: D LANDMAN
ATTN: F GUIGLIANO
ATTN: R BIGONI
ATTN: R DANA
ATTN: R HENDRICK
ATTN: S GUTSCHE
ATTN: TECH LIBRARY

PACIFIC-SIERRA RESEARCH CORP
ATTN: E FIELD

PACIFIC-SIERRA RESEARCH CORP
ATTN: M ALLERDING

ROCKWELL INTERNATIONAL CORPORATION
ATTN: J AASTERUD
ATTN: TECH LIBRARY

S-CUBED
ATTN: C NEEDHAM

SCIENCE APPLICATIONS INTL CORP
ATTN: C SMITH
ATTN: D SACHS
2 CY ATTN: L LINSON

SPARTA INC
ATTN: K COSNER

SRI INTERNATIONAL
ATTN: W CHESNUT

TELEDYNE BROWN ENGINEERING
ATTN: J FORD

TOYON RESEARCH CORP
ATTN: J ISE

VISIDYNE, INC
ATTN: J THOMPSON
ATTN: W SCHLUETER